Organic Fouling Behavior In Nanofiltration Membranes For The Removal of Per- and Polyfluoroalkyl Substances

by

Amy Deringer

A Thesis Submitted in

Partial Fulfillment of the

Requirements for the Degree of

Master of Science

in Engineering

at

The University of Wisconsin-Milwaukee

August 2024

ABSTRACT

Organic Fouling Behavior In Nanofiltration Membranes For The Removal of Per- and Polyfluoroalkyl Substances

By

Amy Deringer

The University of Wisconsin-Milwaukee, 2024
Under the Supervision of Professor Yin Wang

Per- and polyfluoroalkyl substances (PFAS) contamination in drinking water has increasingly become a focus of concern for health and environmental agencies around the globe. Increasing awareness of the detrimental health effects in organisms and humans as well at the bio-accumulative and persistent nature of these “forever chemicals” in the environment has reached drinking water regulations with many governing agencies enacting strict treatment regulations. These new and developing treatment regulations have spurred interest in the development and application of nanofiltration membranes as a possible treatment method for PFAS contamination in source waters. Nanofiltration has shown initial propensity as a viable and effective treatment method.

The main concern in utilizing nanofiltration as a treatment method is the risk of membrane fouling. Fouling decreased the membrane flux, reducing the membrane efficiency and lifespan. In particular, fouling caused by natural organic matter (NOM) is a major concern when applying nanofiltration for PFAS removal. Not only does NOM cause severe fouling, it has the potential to affect specific interaction between PFAS, NOM, and the membrane itself by impacting membrane surface charge, hydrophilicity, functionality, and morphology.

This study compared a commercially available NF270 nanofiltration membrane and a lab synthesized Covalent Organic Framework (COF) nanofiltration membrane with the purpose of analyzing the fouling behavior and mechanisms.

To

Tuna and Yams, my 4-legged study buddies

TABLE OF CONTENTS

LIST OF FIGURES

LIST OF TABLES

LIST OF ABBREVIATIONS

BSA – Bovine serum albumin

COF – Covalent organic framework

DI – Deionized water

GAC – Granular activated carbon

HA – Humic acid

LMH – Liters per square meter hour

MF – Microfiltration

MWCO – Molecular weight cutoff

NF – Nanofiltration

NOM – Natural organic matter

PAC – Powdered activated carbon

PFAS – Per and polyfluoroalkyl substances

PFCAs - Perfluorinated carboxylic acids

PFOA – Perfluorooctanoic acid

PFOS – Perfluorooctane sulfonate

RO – Reverse osmosis

SA – Sodium alginate

UF – Ultrafiltration

ACKNOWLEDGMENTS

The journey to complete this thesis and my master's degree was long and difficult. For all his help and assistance along the way, I would like to thank Dr. Yin Wang. As my advisor over the years his contribution was imperative to my degree fulfilment. I would also like to thank Dr. Thanh Nguyen and Rahul Khandge for their assistance with my research, for answering all my questions, and synthesizing the membranes used in this study. I would also like to thank Dr. Xiaoli Ma and Dr. Qian Liao for serving on my thesis committee and providing their input and feedback on my thesis. I would also like to thank my boss and colleagues for supporting me through this endeavor. Finally, I would like to thank The Bureau of Reclamation's Desalination and Water Purification Research Program (R21AC10025) for providing the funds for this research.

Chapter 1: Introduction

1.1 PFAS contaminants and drinking water treatment

Per- and polyfluoroalkyl substances or PFAS were created in the 1930s and were widely used since the 1940's. [28, 20, 10, 19] PFAS were manufactured on a wide scale for industries such as paper, textiles, pesticides, leather, medical, oil, minerals, metal plating, firefighting foams, and aerospace technologies among many others. Additionally, there are a number of consumer applications for PFAS as well. These included food packaging, cosmetics, personal care products, paints, inks, non-stick cooking utensils, surfactants, and numerous waterproof products. [8, 28, 10, 9, 13]

These synthetic organic compounds were so widely used because of their advantageous chemical structures. They are a diverse class of chemicals that have an aliphatic carbon backbone with hydrogen atoms that are either completely or partially replaced by fluorine. They can be divided into different types based on their carbon chain lengths and functional head groups. The carbon chain length groups are long chain, short chain, and ultra-short chair. The functional head groups are sulfonate, carboxylate, ethyl, and propyl. PFAS structures have a hydrophobic fluorinated alkyl chain at one end and a hydrophilic functional group at the other. [9, 13] Their structures consist of strong carbon-fluorine covalent bonds giving them a unique high thermal and chemical stability. [8, 28, 30, 10, 9, 11, 13] At atmospheric conditions, most PFAS exist as a crystalline or a powder. Shorter chain PFAS with carbon tails ranging from 4-6 appears to exist as a liquid. [3] Only a few compounds have been experimentally measured for solubility in water including perfluorinated carboxylic acids (PFCAs), perfluorooctane sulfonate (PFOS), and fluorotelomer alcohols. [5] PFAS can aggregate into micelles and hemi-micelles if present in

high enough concentrations. [3] Combined, the hydrophobic and lipophobic moieties as well as unique physical and chemical properties complicate the treatment of these substances in water.

The use of PFAS across numerous industries resulted in prolonged exposure to PFAS in humans, wildlife, and the environment. Occupational studies conducted in the 1970's noted detections in the blood of exposed workers. Additional studies in the 1990's detected PFAS in the blood of the general human population. [38] The extent of the environmental fate and occurrence as well as the health effects of PFAS is still being explored and has resulted in a sleuth of studies to determine the extent and impact of PFAS. It is now known PFAS are essentially ubiquitous in nearly all aquatic matrices including drinking water, wastewater, groundwater, surface water and coastal water. [19] Following these studies, extensive studies measuring the risks of PFAS exposure to human health and ecological environment have gained more attention. [11, 13, 3]

Numerous studies suggest the potential toxicity of PFAS and interference with the endocrine system and its function, cell information transmission, and normal protein function. [28,20,5,19, 13] In addition, the bioaccumulative nature of PFAS was noted in many studies. [19, 3] The potential amplification effect on the biological food chain is not fully understood. However, their ability to withstand degradation under natural conditions implies a significant amplification effect, thus increasing the urgency to develop effective treatment methods.

Various jurisdictions across the globe, such as the Persistent Organic Pollutants Convention are working to limit or ban PFAS use and production. [8, 5, 13] However, some critical industries do not have suitable substitutes to PFAS and therefor it is not possible to eliminate their use completely. For example, PFAS-containing firefighting foams have been highly

effective for extinguishing high-heat liquid fuel fires specifically due to their unique chemical properties. [28] Instead, production of PFAS in countries like the US and Europe has become increasingly regulated.

1.2 Treatment methods

A number of existing and novel treatment methods have been explored for PFAS removal in drinking water. Conventional water treatment processes including coagulation, flocculation, precipitation, and activated sludge processes have a very limited ability to remove PFAS from water. They are generally considered invalid designated methods for PFAS removal. [7] Advanced treatment processes like electrocatalysis, photocatalysis, and oxidation-reduction can effectively decompose PFAS, but require very specific reaction conditions and high energy consumption.[13] Because of this, these methods are neither convenient nor economical nor energy efficient enough to remove trace amounts of PFAS from source water. Membrane processes have since emerged as the possible solution for PFAS treatment. Membrane separation processes have the potential characteristics of high removal efficiency, low energy consumption, simple operating procedures, manageable cost, and low pollution output. [13, 19,]

1.2.1 Conventional Treatment Methods

The high hydrophobicity of PFAS makes them unlikely candidates for removal by conventional coagulation, flocculation, and sedimentation processes. A study in Kansai Japan showed there was no difference in PFAS concentration between plant influent and sedimentation unit effluent samples. [39] Many studies found essentially no PFAS removal by coagulation and sedimentation nor sand filtration proceeded by sedimentation.[13, 19, 11] Studies conducted on

surface, ground, and drinking water found that both rapid and slow sand filtration are unlikely to be effective for PFAS removal. In some cases, detected concentration of perfluorooctanoic acid (PFOA) and PFOS in treated waters was higher than detected concentrations prior to treatment. [4] Furthermore, oxidation processes are not effective methods of PFAS treatment due to fluorine being one of the most electronegative elements. Therefore, PFAS are resistant to oxidation and retains their electrons.

Granular activated carbon (GAC) adsorption is widely used in drinking water treatment plants to reduce the concentration of synthetic organic contaminates, taste and odor compounds, and NOM. GAC filters have had limited successes in treating PFAS. Studies of five treatment plants in Osaka Japan found that when new or in use for less than nine months, GAC filters could achieve 69-100% removal of PFOS and PFOA at the ng/L level. [39] It was also found that GAC filters alone were effective in removing PFAS in treatment plants and not the preceding processes such as coagulation, rapid sand filtration, and ozonation. Again, the effectiveness of GAC filters varied for specific PFAS and generally failed to remove shorter chain PFAS such as PFBA, PFBS, PFPA, and PFHxA. [40] Furthermore, it was found that branched isomers were less sorbable to GAC compared to linear isomers. Desorption from GAC filters in use for long periods was also observed. [4]

Powdered activated carbon (PAC) systems have also been studied for PFAS removal. PAC is favored in water treatment plants for removal of micro pollutants but the operation of these systems is costly and complicated. Their application to short and long chain PFAS at varying concentrations has been explored and showed higher adsorption capacity due to the materials greater surface area, shorter internal diffusion, higher site accessibility, and increased adsorption kinetics as compared to GAC.[34] In fact, high removal efficiency for both short and

long chain PFAS was achieved even at low concentrations and in source waters with high concentrations of dissolved organic carbon which typically reduces PFAS adsorption capacity. [34]

1.2.2 Low Pressure Membranes

Low pressure membranes are typically used to remove particulates, colloids, and viruses from water. Their application to PFAS treatment in aqueous environments has been explored because of their ability to yield higher permeate flux and significantly lower operating costs compared to high pressure membranes.[13] Low pressure membranes include Microfiltration (MF) membranes which range in size from 0.1 to 5 microns and Ultrafiltration (UF) membranes which range in size from 0.01 to 0.1µm. It is largely believed that MF and UF membranes alone are ineffective at removing PFAS and other dissolved constituents. This is due to pore size and the size of PFAS molecules. The effective diameter of these PFAS molecules is around 1 nanometer; smaller than the low pressure membrane pore size which is around 100 nanometers in MF systems and 20 nanometers in UF systems. Without surface modification, MF and UF membranes remain ineffective treatment methods. Much of the literature available today shows that despite the limited success shown in utilizing surface modified UF membranes, MF and UF membranes are more suited for use in the treatment chain approach as pre or post treatment system for PFAS removal in conjunction with other adsorbents or membranes rather than being employed as a sole treatment method. [27]

1.2.3 High Pressure Membranes

High Pressure membranes include Reverse Osmosis membranes and Nanofiltration membranes. High pressure membranes are an emerging technology applied to PFAS treatment. In these systems, a pressurized feed stream is fed across the membrane allowing for selective permeation across the membrane to occur. This produces a mainly solute permeate. PFAS molecules that are larger than the membrane pore size are rejected by the barrier layer and removed from the membrane through the reject stream or retentate. The relatively smaller pore size allows for significantly greater PFAS removal rates than seen in low pressure membranes. Membrane characteristics such as material, pore size, and surface charge will impact the physicochemical interactions between PFAS and membranes which alters the PFAS rejection of a given membrane. Membranes and pore size as well as molecular weight cutoff (MWCO) plays the most important role in the rejection of PFAS by high pressure membranes. The pore size of the permselective layer of the membrane dictates the membranes PFAS retention performance primarily through the steric or size exclusion. Reverse Osmosis and Nanofiltration generally utilize a cross-flow configuration to avoid the accumulation of solutes on the membrane system.

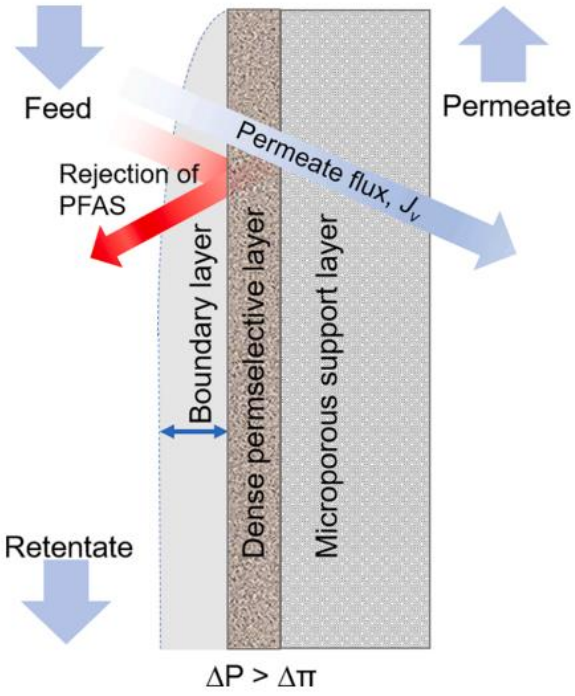

Figure 1. Cross-flow membrane filtration [16]

1.2.3.1 Reverse Osmosis (RO)

Reverse Osmosis (RO) membrane technology is already widely used in seawater desalination, drinking water production, brackish water treatment and wastewater treatment. [35] Because of their widespread use in desalination, RO membranes are an attractive test material for studies exploring PFAS removal technologies. These polyamide RO membranes are characterized by the pore size smaller than 1 nanometer and are typically comprised of three layers. The first layer is a pH resistant, rough, and slightly negative semi permeable membrane made of polyamide with hydrophilic properties. The second layer is the structural support for the first layer and is comprised of poly-sulfone. The third layer provides further support and stiffness to the membrane and is made of a nonwoven polyester fabric. [32] This dense structure has

afforded these membranes significant initial successes in removing PFAS and has shown higher observed rejection for PFAS compared to other membrane filtration technology. [28]

RO membranes use three main mechanisms to remove PFAS. These mechanisms include size exclusion, charge repulsion, and adsorption or diffusion. Size exclusion, also known as straining, is the dominant rejection mechanism in RO membranes. Due to the small pore size, RO membranes allow water molecules to pass through while blocking larger molecules like salts and larger PFAS molecules. A good predictor of size exclusion is the molecular diameter or width of a molecule. However, studies have investigated if molecular weight and MWCO could be reliable predictors of chemical rejection. [32] The MWCO for RO membranes is generally 98-100 daltons. It was found however, that not all chemical molecules rejected by the RO membranes had molecular weights higher than the MWCO.[32] The second exclusion mechanism is charge repulsion. The presence of carboxylate functional groups in the polyamide membrane layer causes a negatively charged membrane surface which allows for charge repulsion to occur. This charge repulsion allows the polyamide RO membrane to remove negatively charged solutes including PFAS. Adsorption and diffusion are driven by hydrophobic interactions. Adsorption of hydrophobic molecules onto the RO membrane is generally expected to decrease the rejection rate of similar molecules due to concentration enrichment. The limited number of adsorption sites in polyamide membranes reduces the impact of hydrophobic interactions, suggesting size exclusion and charge repulsion are dominant removal mechanisms.

1.2.3.2 Nanofiltration (NF) Membranes

Nanofiltration is a pressure driven membrane-based separation process widely used in water and wastewater treatment. NF membranes are characterized by a pore size ranging

between 1 and 10 nanometers and show higher water permeability than RO membranes of pore size less than 1 nanometer. [17, 31]The MWCO and pore size of NF membranes used for PFAS treatment tend to be in the range of 90-1000 Da and 0.3 - 2.1 nm. [17] The larger MWCO allows water molecules to cross the membrane pores more easily. There are several commercially available membranes that have been utilized to remove PFAS. The majority of commercially available NF membranes are thin film composite membranes consisting of three components. The first being a nonwoven polymeric support. The second is a microporous polymeric support. The third component is a thin separation layer consisting of cross-linked polyamide. These commercially available membranes are generally negatively charged. The two most common are NF90 and NF270, both of which have reported removal efficiencies of 90% or greater. Studies on these membranes suggest that greater applied pressure and initial flux, the occurrence of fouling increased along with the PFOS rejection rate increasing to 90-99% removal. [9, 28, 33, 5, 11, 19, 13]

Similar to RO membranes, PFAS removal mechanisms of NF membranes are primarily size or steric exclusion and electrostatic interactions. Size exclusion again is due to the pore size of the membranes. Specifically, the NF membranes pre selective layer determines the PFAS retention performance. Because of the very small pore size, PFAS groups like PFOA, which have a relatively high molecular weight of 414 g/mol, can be retained by NF membranes through size exclusion. [33] Generally, the removal of both PFCA and PFSA by NF membranes is not closely related to its molecular weight. In fact, the NF membrane pore size and MWCO have a negative correlation with PFAS removal. [17, 32] Although some literature has drawn conclusions that the MWCO can affect the rejection of PFAS in bench scale tests, it was also found that similar to RO membranes, when MWCO of the membrane is lower than the PFAS

molecular weight a better retention effect can be achieved. This suggests that steric exclusion plays a dominant role in PFAS rejection but is not the exclusive separation mechanism. [17, 32] In fact, basic membrane characteristics could influence PFAS rejection significantly. Transport properties, salt rejection, and surface charge all play a unique role in PFAS rejection.

One study suggests that PFAS removal had a negative correlation with water permeability coefficients and less permeable membranes were effective at excluding PFAS and salts. [17] Similar to RO membranes, the negative surface charge of NF membranes played a critical role in removing PFAS which are mostly negatively charged. [17, 32] Previous studies suggested that the charged carboxyl functional groups on the surface of the polyamide membrane could enhance the electrostatic exclusion between the membrane and negatively charged solute, such as PFAS anions, thus contributing to PFAS removal. Additionally, electrostatic repulsion was found to be a dominant rejection force by NF membranes. [31]

1.3 COF membranes

Covalent organic frameworks (COFs) are a novel class of porous materials with predictable well defined crystalline networks. These materials are comprised of periodically extended and covalently bound crystalline porous network structures. They are synthesized from organic linkers utilizing a reversible covalent bond. [12] Assembly via this method allows for orderly arrangement of pores, uniform pore size, and high pore density, making them promising materials for advanced separation membranes. [23] Their high specific surface area and well-developed porosity make them highly efficient adsorbents for a wide range of pollutants due to their increased selectivity and porosity. COFs have been looked at for PFAS removal because of their adaptable surface hydrophobicity, optional F-F affinity, modifiable functional groups, and

wide range of pore shapes and sizes. [12, 23] COFs can be easily synthesized through dynamic covalent bonding and therefore are highly suitable for studying the adsorption mechanisms of pollutants on porous adsorbents. Currently, the utilization of COF membranes as effective and efficient adsorbent membranes for addressing environmental issues remains limited. [7]

The crystallinity of COF membranes is highly dependent on the proper design of their organic building blocks and allows for precise arrangements of functional groups with a strong affinity for PFAS. COF adsorption capacity for PFAS can be improved through establishing electrostatic interactions between functional groups, adding fluoro-functional groups to enhance F-F affinity, increasing hydrophobic interactions, and achieving high specific surface area to establish the proper pore size for selective adsorption. [23] Many variables in membrane technology can impact the separation performance of membranes. COF membrane surface properties like hydrophilicity or hydrophobicity, surface charge, and proton conductivity can also have significant influences on the membrane performance [8]

The structure-activity relationship between the adsorption of PFAS and pore size in COF membranes is not yet fully understood. Further, while previous studies have demonstrated the performance of COF adsorbents for PFAS removal, limited work has focused on the development of COF membranes for PFAS treatment. More research in this area could enhance the PFAS removal efficiency. [7] Overall, the low density and large surface area structure of COFs are highly advantageous. In addition, the tunable pore size and structure facilely-tailored functionality as well as versatile covalent-combination of building units have increasingly made COF membranes a focus of study for the improvement of membrane technology for PFAS removal. [12]

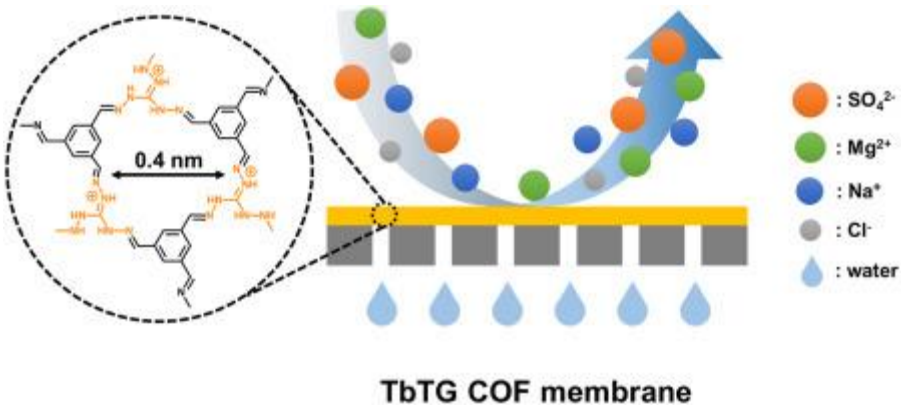

Figure 2. COF membrane structure taken from [16]

1.4 Membrane Fouling

Membrane fouling can be defined as the deposit and accumulation of materials on the membrane surface or inside the membrane pores, causing a decrease of permeation flux. [36] In general, fouling can be divided into surface and internal fouling. Low pressure membranes like MF and UF membranes have different dominant fouling mechanisms from high pressure membranes like RO and NF membranes. MF and UF membranes more commonly foul through pore adsorption and clogging while surface fouling is more common for RO and NF membranes. However, the relatively compact and nonporous nature of RO membranes allows for more frequent fouling as compared to MF and UF. [30]Neither fouling option is "better" however surface fouling is more easily controlled through improving feed water hydrodynamic conditions and chemical cleaning. [30] Because surface fouling can be controlled more easily, it can be more reversible than internal fouling. Regardless, both surface and internal fouling can be irreversible.

Fouling can be further classified into biofouling, organic fouling, inorganic scaling, and colloidal fouling. Biofouling occurs when microorganisms adhere, and grow on the membrane

surface. A biofilm forms to an extent that it interferes with operations. [30] Organic fouling is the accumulation of carbon-based material on a membrane. Inorganic scaling is induced by supersaturation of mineral ions due to continuously increasing concentration.[44] The focus of this study is organic fouling which is caused by organic matter. Typical organic fouling materials include lipids, nucleic acids and amino acids, organic acids, cell component, and the three featured in this study, humic substances, polysaccharides, and proteins. Fouling typically occurs on the membrane surface by depositing on the surface through foulant-surface interactions followed by foulant-foulant interactions causing more foulant to deposit on the membrane surface resulting in serious membrane fouling. Fouling can intensify when combined with other foulants due to foulant-foulant interactions. Fouling can lead to pore plugging and cake formation, leading to a cake enhanced concentration polarization. Then through electrostatic interactions, the cake layer can then act as a secondary membrane, further increasing the rejection rate. Fouled membranes exhibited greater rejection efficiencies than new membranes particularly for PFAS with smaller molecular radiuses.

Natural organic matter (NOM) can form a fouling layer on the membrane surface that alters membrane porosity morphology and surface chemistry thereby affecting PFAS retention. [17] Studies focused on PFAS removal in the presence of NOM fouling look to determine the effectiveness of the NF removal from water. The implicit goal is to identify the main factors impacting either PFAS adsorption or transmission during NOM fouling. [17] Exploring specifically the presence of bovine serum albumin (BSA), sodium alginate (SA), and humic Acids (HA), it has been suggested that the presence of NOM can significantly aggravate membrane fouling but varied depending on the type of NOM. [17] It is also suggested that alginate imparts the most significant fouling propensity followed by humic substances while

proteins present the least fouling potential. The fouling behaviors could be mainly attributed to different propensities of carboxylic acids in BSA, HA, and SA. [17] When the deposition of SA on membrane surface gradually increased its rough surface carboxylic acids and large molecular weight could trap the calcium ions in feed solution to form a more serious concentration polarization phenomenon, causing a significant flux decline. These results also suggest that the existence of PFAS would not alter NOM fouling trend among BSA, SA, and HA. [17]

One factor impacting membrane fouling is the molecular weight of organic matters. Lower molecular weights are more difficult to remove through conventional pretreatment technologies. Studies suggest initial stages of fouling were caused by medium to low molecular weight, yet a majority of fouling was caused by high molecular weight organic matters.

1.5 Membrane Cleaning and Flux Recovery

Because fouling has a significant impact on the performance of membranes, there are two strategies deployed to minimize the effect of fouling. These can be classified into two major groups: minimization and remediation.

By utilizing pretreatment methods, it is possible to avoid or control fouling to a certain degree. Coagulation followed by filtration and sedimentation can be used as an effective pretreatment method, however its effectiveness is largely dependent on the raw water quality specifically its organic and inorganic suspended particulate matter. Factors such as flow rate, backwash frequency, and pH in the pretreatment process will have an impact on the effectiveness. One study concluded that, a coagulant treated water could decrease the fouling after prefiltration, suggesting that coagulated particular matter can form a dynamic layer material on membrane surfaces. [37]

Membrane prefiltration and membrane modification are also a viable option. As discussed above the application of MF and UF as NF prefilters has become a promising method in pretreatment to minimize fouling.

1.6 Goals and Objectives

This study focused on the fouling behavior and mechanisms of natural organic matter. It is well known and established that NF membranes are highly efficient and effective at removing PFAS from source water. However, there is currently limited information and research focusing on the impact of NOM on PFAS rejection in NF membrane processes. It is also known that NOM is a significant contaminant in water treatment processes which causes sever membrane fouling and directly impacts the removal efficiency of coexisting micropollutants. [18] NOM contamination is likely to cause changes in surface charge, hydrophilicity, functionality, and morphology; all of which have the potential to affect PFAS/NOM interactions.

By first studying the fouling mechanism of NOM in commercial and novel COF membranes, initial conclusions about the dominant fouling mechanism can be drawn and compared and the impact on PFAS/NOM interaction can be speculated. Therefore, this study aimed to compare the fouling mechanisms of the commercially available DuPont NF270 nanofiltration membrane and a lab synthesized COF nanofiltration membrane. Foulant concentration, feed water chemistry, pressure, and flow rate remained constant while foulant and membrane varied by experimental run. Analysis was conducted on the average fouling rate and single and combined fouling mechanisms. Physical cleaning of both membranes under all fouling conditions was tested and the flux recovery was analyzed.

1.7 Organization

Chapter 1 reviewed literature on pressure-driven membrane systems for removing PFAS in drinking water. The research goals and objectives were also provided in chapter 1. Chapter 2 covered the materials and experimental methodology. Chapter 3 covered the experimental results and discussion. Chapter 4 covered the study's conclusions as well as recommendations for future work.

Chapter 2: Materials and Methodology

2.1 Overview

Membrane separation technology has many applications in various industries including biotechnology, pharmaceuticals, desalination, drinking water and wastewater treatment, among many others. MF, UF, RO, and NF have been successfully deployed in water treatment efforts though efforts for technological improvements have largely focused on RO and NF. [27] The ability of these membranes to efficiently remove naturally occurring organic matter from source waters have put these membranes at the forefront of PFAS treatment in drinking water with applications in wastewater anticipated to follow. NF membranes are unique in their ability to be tailored to specific systems. Low pressure selectivity, high permeability, and retention of beneficial trace elements all contribute to the adaptivity of NF membranes. The main concern with using NF membranes is the inevitable membrane fouling which increases the differential pressure across the membrane and decreases the membrane flux.

2.2 Materials

For this experiment a commercially manufactured DuPont NF270 nanofilitration membrane was used. Additionally, this experiment utilized COF membranes, synthesized by the University of Wisconsin - Milwaukee's Department of Material Sciences and Engineering. Experimental parameters were kept consistent for both membranes.

Both membranes were first prepped by soaking in deionized (DI) water for a minimum of 24 hours prior to testing. The first phase of the experiment was initial compaction in which DI water was used. The second phase of the experiment, called conditioning, included a foulant free

electrolyte solution of 10 mM sodium chloride. The third phase was the fouling phase, which fed a 25 mg/L foulant solution through the system. This experiment used 3 foulants, SA, BSA, and HA. The final phase of the experiment was flux recovery after physical cleaning in which DI water was fed into the system at a flow rate between 0.5 and 0.6 liters per minute.

The experimental set up consisted of a commercially available pump, tubing, and two membrane cells set up in a cross-flow orientation, one pressure gage, two fluid valves, and a flow rate gage (Figure 3). Two beakers were set on two electronic scales below the outflow point of the membrane cell to collect and measure the mass of the permeate throughout the experiment. Data was automatically collected every minute during the experimental run using RS key software. This data was used to calculate the flux and permeance. The membrane cells were kept in the same positions throughout the entire experiment set up. Cell 1 remained in the first position and received feed water first. Cell 2 remained in the second position and was removed prior to physical cleaning and flux recovery.

Figure 3. Experimental set up.

2.3 Experimental Methodology

During the initial phase of the experiments, the membranes were compacted at a constant pressure of 100 psi for 24 hours with pure DI water. COF membranes were compacted at this same pressure with DI water, but for 48 hours after it was found that the flux did not reach stability in 24 hours.

During the second phase of the experiments, membranes underwent conditioning and were fed a foulant free electrolyte solution of 10mM sodium chloride at a constant pressure of 80 psi for 24 hours to create a conditioning baseline. The conditioning phase did not differ between membrane types.

In the third phase of the experiments, a fouling solution was added. The fouling solution consisted of 150 ml of the stock solution into 3 liters of the 10mM sodium chloride solution, providing a final foulant concentration of 25 mg/L. Each foulant was tested individually in both membranes. The three foulants were also combined and tested in both membranes. The fouling solution for this consisted of 50 ml of stock solution from all 3 stock solutions, totaling 150 ml of stock solution into 3 liters. The pressure in phase three was held at 80 psi like in the conditioning phase of the experiments. The fouling phase was run for 48 to 72 hours per membrane.

Finally, in the last phase, the cell in the second position was removed and the used membrane saved. The first membrane in line underwent physical cleaning with DI water, during which DI water was fed through the system under no pressure but at a flow rate between 0.5 and 0.6 liters per minute for one hour. The DI water was then replaced and fed through the system for 24 hours at 100 psi for flux recovery.

Total experiment run time for NF270 membranes was 144 hours. Total run time for COF membranes was 168 hours. For all phases, the temperature was held at room temperature. Mass of the permeate was recorded and used to calculate the instantaneous flux and water permeance using the following equations:

$$Flux\ (Ji) = \frac{\Delta\ Mass\ (g)}{1000} \div (\frac{1}{60} \times Membrane\ Surface\ Area\ (m2)) \quad (1)$$

$$Water\ Permeance = \frac{Flux}{Pressure} \quad (2)$$

2.4 Modeling

After the experiments were conducted, the actual volume collected during the fouling phase was compared to the theoretical volume based on the theoretical single (Table 1) and combined (Table 2) fouling mechanism models developed by [25] and [26]. The theoretical single fouling mechanism models included the standard blocking model, complete blocking model, intermediate blocking model, and the cake filtration model. The theoretical combined fouling mechanism models included the cake complete model, cake intermediate model, complete standard model, intermediate standard model, and the cate standard model. The sum squared residuals (SSR) or model fit error and model fit variance was calculated for each experimental condition and theoretical model. Based on the model fit variance, the best fit theoretical model was determined and presumed to be the dominant fouling mechanism.

Table 1. Single Fouling models. [25][26]

Model	Equation	Fitted Parameters
Complete blocking	$V = \frac{J_0}{K_b}(1 - e^{K_b} b^t)$	K_b (s^{-1})
Intermediate blocking	$V = \frac{1}{K_i}\ln(1 + K_i J_0 t)$	K_i (m^{-1})
Standard blocking	$V = (\frac{1}{J_0 t} + \frac{K_s}{2})^{-1}$	K_s (m^{-1})

Cake filtration	$V = \frac{1}{K_c J_0}(\sqrt{1 + 2K_c {J_0}^2 t} - 1)$	K_c (s/m^2)

Table 2. Combined Fouling models. [25][26]

Model	Equation	Fitted Parameters
Cake complete	$V = \frac{J_0}{K_b}(1 - e^{\frac{-K_b}{K_c {J_0}^2}\left(\sqrt{1+2K_c {J_0}^2 t}-1\right)})$	K_b (s^{-1}) K_c (s/m^2)
Cake intermediate	$V = \frac{1}{K_i}\ln(1 + \frac{1}{K_c J_0}(\sqrt{1 + 2K_c {J_0}^2 t} - 1))$	K_i (m^{-1}) K_c (s/m^2)
Complete standard	$V = \frac{J_0}{K_b}(1 - e^{\frac{-2K_b t}{2+K_s J_0 t}})$	K_s (m^{-1}) K_b (s^{-1})
Intermediate standard	$V = \frac{1}{K_i} ln(1 + \frac{2K_i t}{2 + K_s J_0 t})$	K_i (m^{-1}) K_s (m^{-1})
Cake standard	$V = \frac{2}{K_s}(\beta \cos\left(\frac{2\pi}{3} - \frac{1}{3}\cos^{-1}(\alpha)\right) + \frac{1}{3})$ $\alpha = \frac{8}{27\beta^3} + \frac{4K_s}{3\beta^3 K_c J_0} - \frac{4{K_s}^2 t}{3\beta^3 K_c}$ $\beta = \sqrt{\frac{4}{9} + \frac{4K_s}{3K_c J_0} + \frac{2{K_s}^2 t}{3K_c}}$	K_s (m^{-1}) K_c (s/m^2)

Chapter 3: Results and Discussion

3.1 Results

For all foulants, a visible foulant layer was observed on the surface of both NF270 and COF membranes, suggesting cake filtration might be the primary fouling mechanism (Figures 4 and 5). However, due to the long run time of the experiment, it is possible that pore clogging occurred before cake filtration and ultimately initiated the membrane fouling.

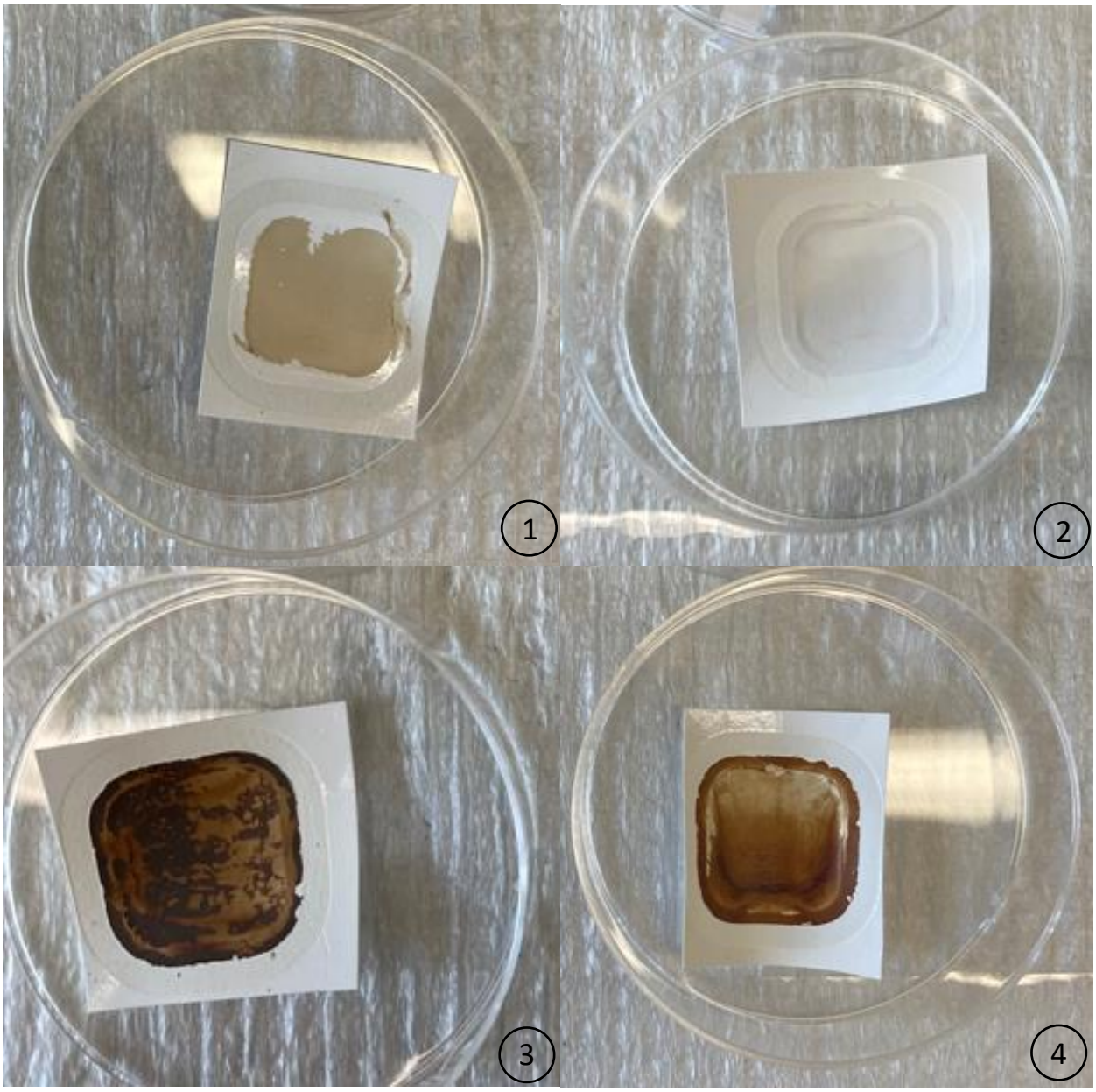

Figure 4. Organic Fouling in NF270 membranes under Sodium Alginate fouling solution (1), BSA fouling solution (2), Humic acid fouling solution (3), and a combined fouling solution (4).

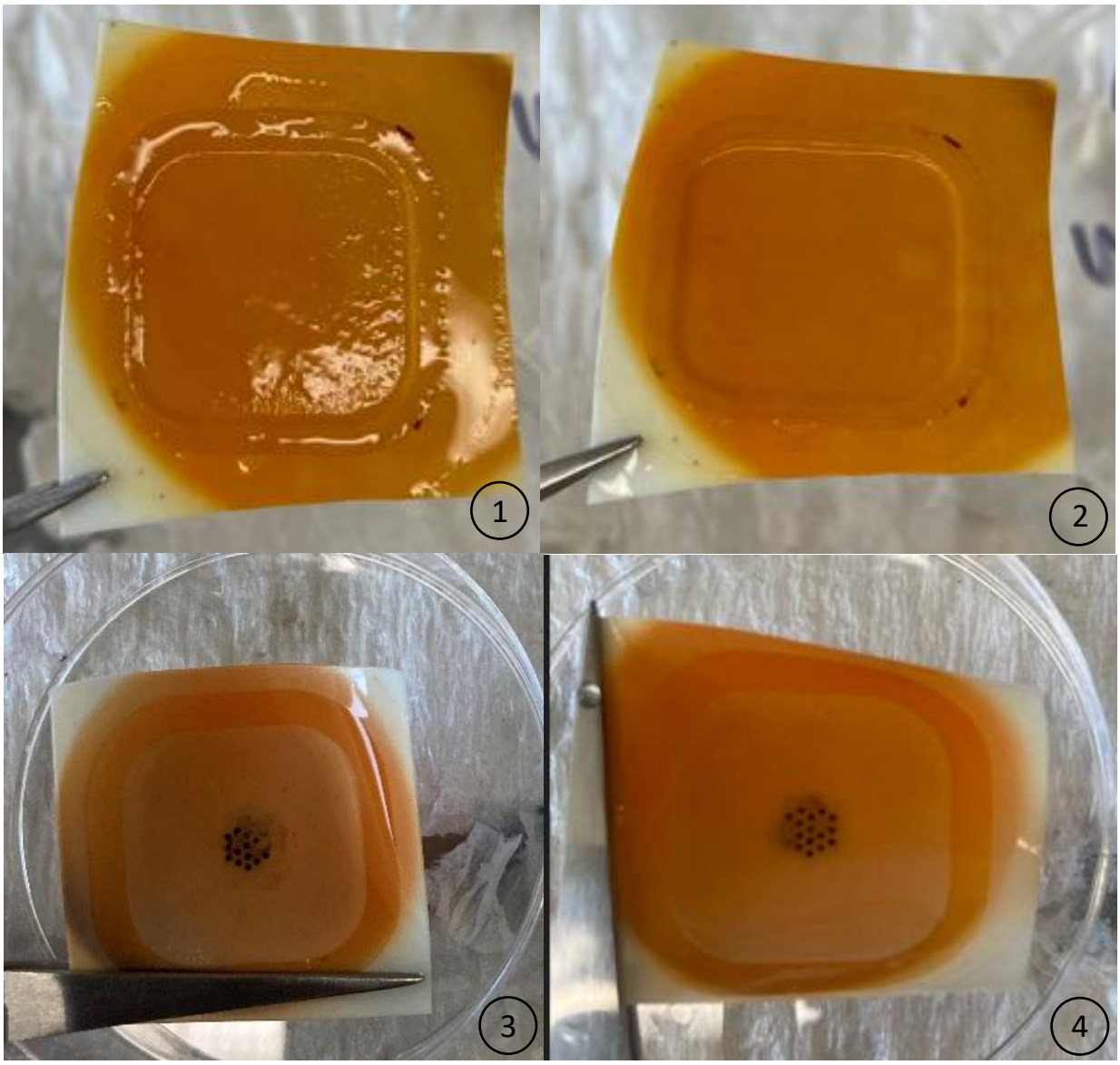

Figure 5. Organic Fouling in COF membranes under Sodium Alginate fouling solution (1), BSA fouling solution (2), Humic acid fouling solution (3), and a combined fouling solution (4).

3.2 Organic fouling in NF270 membranes

The 10-minute average flux was normalized by the maximum 10 minute average flux of each individual run. For SA (Figure 6), a rapid decline in flux was noted during DI water

compaction. A sharp increase in flux was observed between DI water compaction and electrolyte conditioning however flux remained steady throughout conditioning. Following conditioning a steady and gradual decline in flux was observed. Furthermore, physical cleaning exhibited a flux recovery just over 0.2 and near linear decline flux during re-compaction.

For BSA (Figure 7), a rapid near linear decline in flux was noted during DI water compaction. An increase in flux was also observed between DI water compaction and electrolyte conditioning. Flux decreased slightly during conditioning reaching steady in the membrane in the second cell position. Between conditioning and the fouling solution a sharp decreased in flux was observed, and thereafter, a steady decrease in flux was observed until day 3. Day 3 of the fouling solution saw a small increase in flux followed by declining flux until the flux was roughly the same as it was at the end of day 2. Physical cleaning on the BSA fouled membrane did not show any flux recovery.

For HA (Figure 8), a steady decline in flux was observed during DI water compaction. Another sharp increase in flux was observed between compaction and electrolyte conditioning followed by decline in flux. An increase in flux was observed between electrolyte conditioning and the fouling solution, followed by a steady decline in flux until a near steady state was reached near the end of day 3 of the fouling solution. Physical cleaning on the HA-fouled membrane exhibited a flux recovery just over 0.2 and remained steady during re-compaction.

For the combined foulant solution (Figure 9), experimental run one showed a gradual decline in flux during DI water compaction and a sharp decrease in flux between compaction and electrolyte conditioning. Through conditioning and fouling, a gradual decline in flux was observed. After physical cleaning, the fouled membrane exhibited a flux recovery around 0.4 and

remained relatively steady during re-compaction. Experimental run 2 a showed similar near linear decline in flux during DI water compaction. A sharp increase in flux was observed between DI water compaction and the electrolyte conditioning phase. During conditioning and fouling, a near identical decline in flux was observed in these membranes.

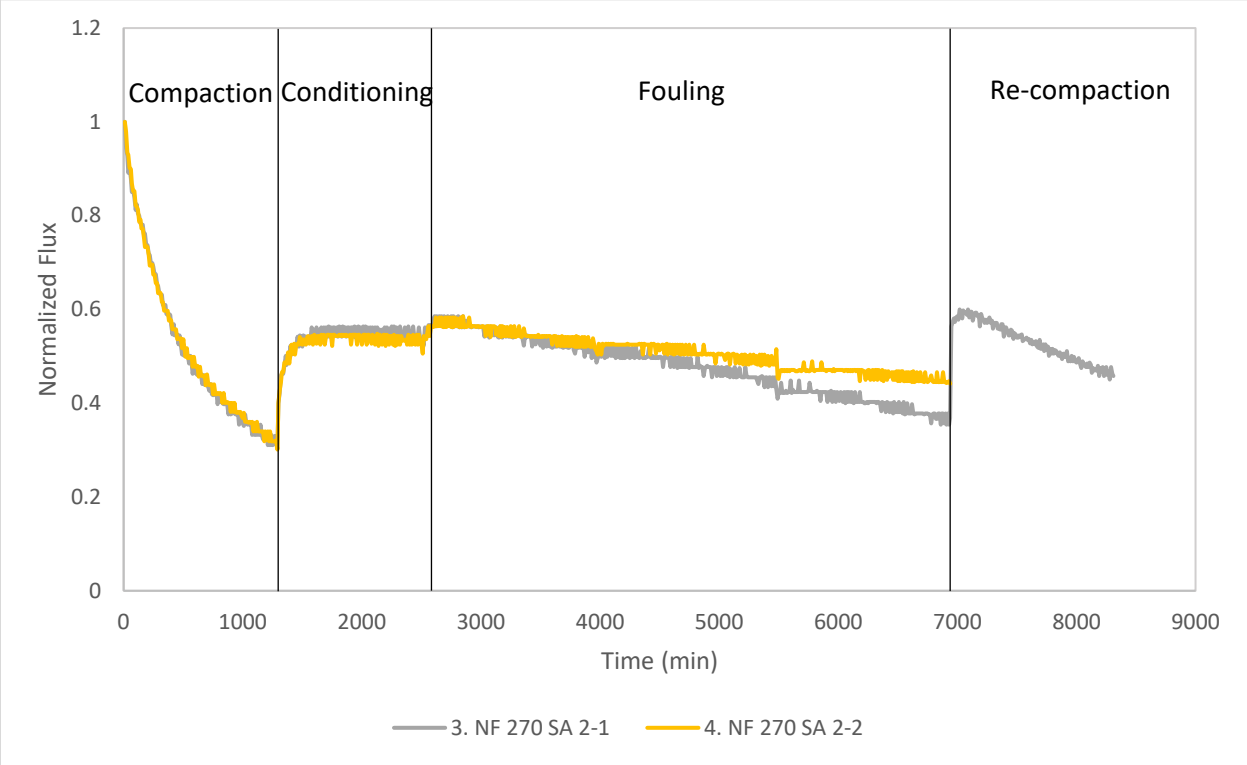

Figure 6. Change in flux over time, normalized by the maximum flux, during organic fouling by 25 mg/L sodium alginate in DuPont NF-270 membranes.

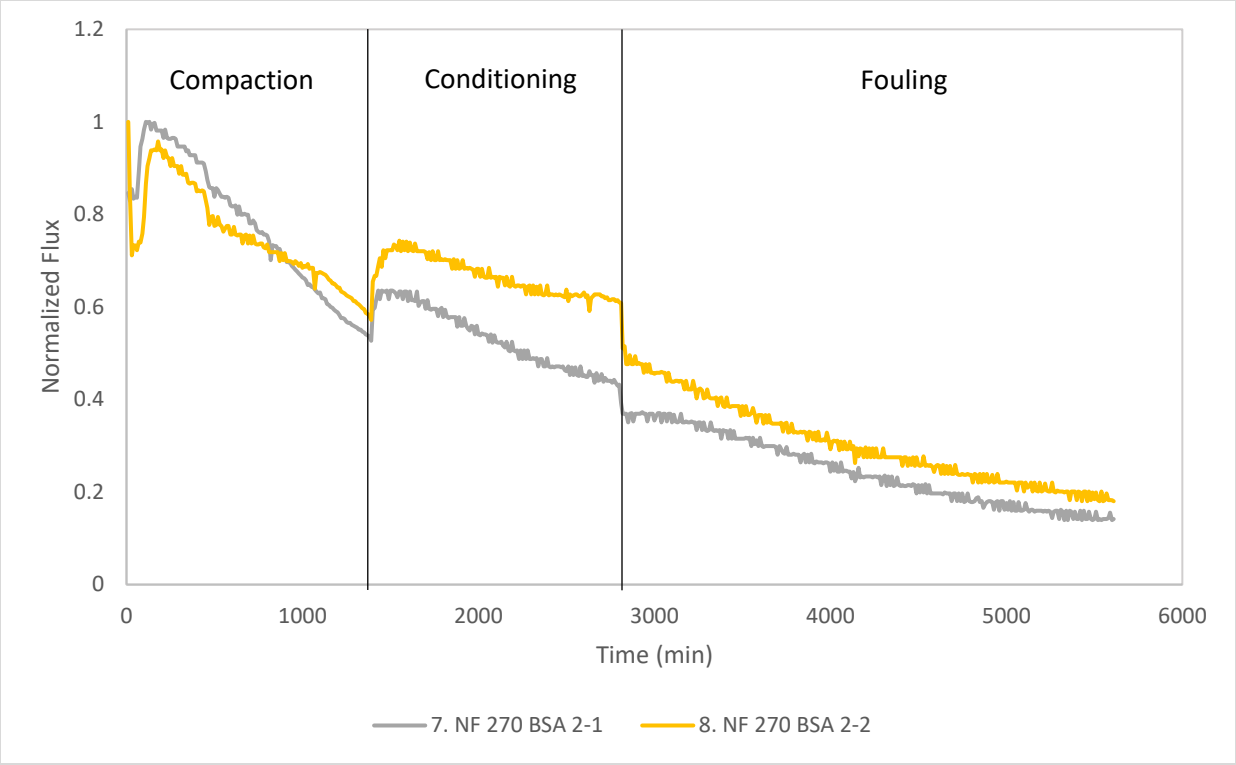

Figure 7. Change in flux over time, normalized by the maximum flux, during organic fouling by 25 mg/L BSA in DuPont NF-270 membranes.

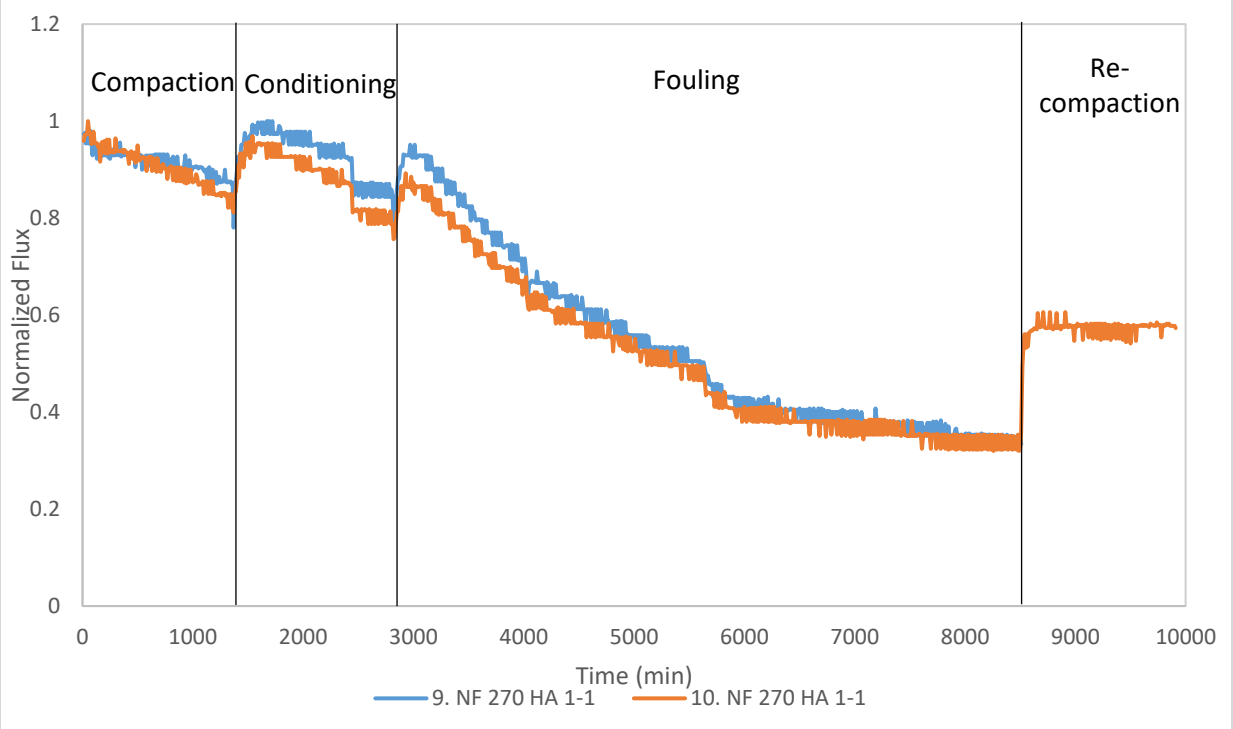

Figure 8. Change in flux over time, normalized by the maximum flux, during organic fouling by 25 mg/L Humic Acid in DuPont NF-270 membranes.

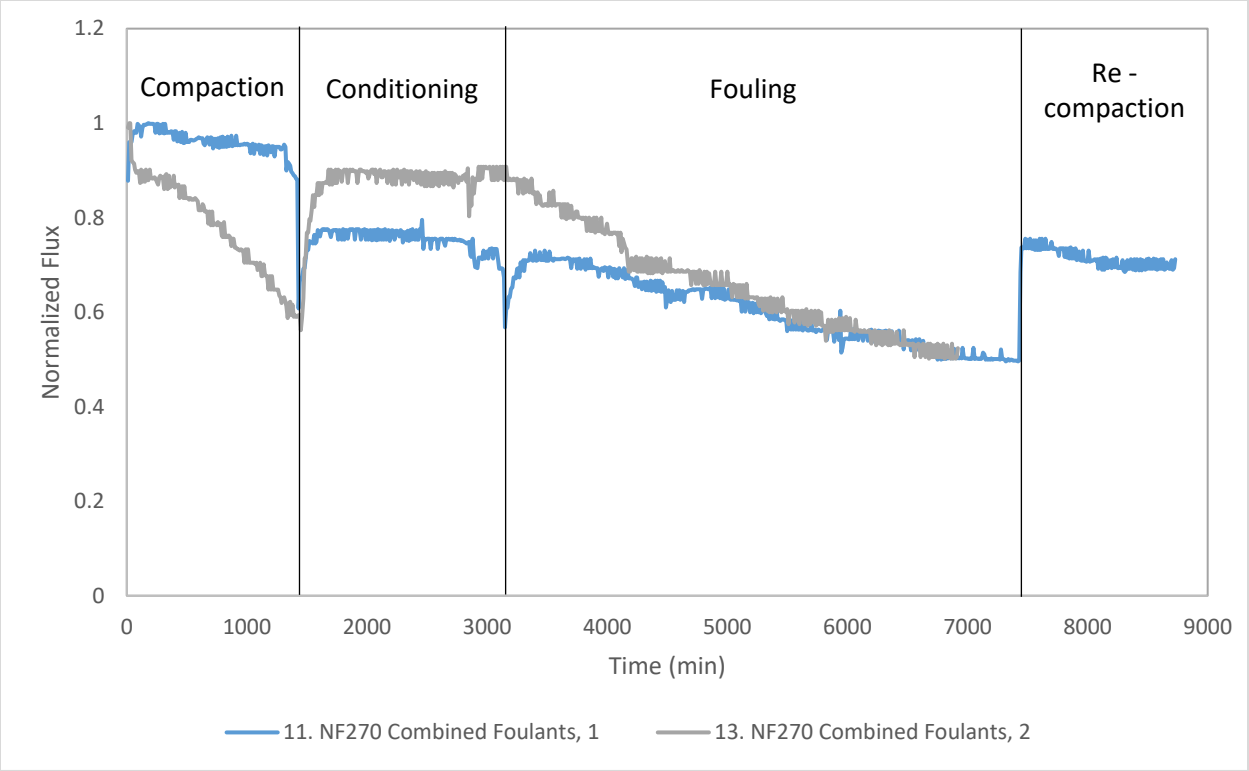

Figure 9. Change in flux over time, normalized by the maximum flux, during organic fouling by 25 mg/L Combined foulant solution in DuPont NF-270 membranes.

3.3 Organic fouling in COF membranes

The 10-minute average flux was normalized by the maximum 10-minute average flux of each individual run. The COF membranes used in this experiment were low flux COF membranes.

For SA (Figure 10), the membranes saw immediate rapid decline in the 10-minute average flux during the DI water compaction phase and did not reach a steady state prior to electrolyte conditioning. The 10-minute average flux remained at a steady state throughout electrolyte conditioning. During fouling phase, the 10-minute average flux declined slightly during day one and then increased slightly on day two of fouling and then remained steady

through the final day of fouling. After physical cleaning, the flux increased slightly and remained steady.

For BSA (Figure 11), the membranes saw immediate rapid decline in the 10-minute average flux during the DI water compaction phase eventually reaching a steady state roughly halfway through the DI water compaction phase. The sharp decrease of flux during COF membrane compaction might be related to unknown sources of contamination of the system. The exact mechanisms are still not fully understood and require further investigation. The 10-minute average flux remained at the steady state throughout the remainder of the experimental run, possibly suggesting no fouling was observed after the compaction phase. Physical cleaning of the BSA fouled membrane appeared to have no significant results.

For HA (Figure 12), the membranes experienced a more gradual decline in the 10-minute average flux during the DI water compaction phase eventually reaching a steady state near the end of the 2-day compaction phase. The flux appeared to have decreased during the electrolyte conditioning phase but reached steady state quickly. Similarly, the flux decreased during the fouling solution quickly and remained steady during those 3 days. Physical cleaning showed a small flux recovery which remained steady through re-compaction.

For the combined fouling solution, flux decline in the DI water compaction phase was more gradual than the other fouling solutions and eventually reached a steady state near the end of day 2. A sharp decline in flux was observed between DI water compaction and electrolyte conditioning. Flux remained steady in the electrolyte conditioning phase. Another sharp decline in flux was observed between electrolyte conditioning and the fouling solution phase. Flux in the fouling phase reached a near steady state at the end of the first day and remained there for the

remaining days. Physical cleaning of the combined foulant solution fouled membrane appeared to have no significant results.

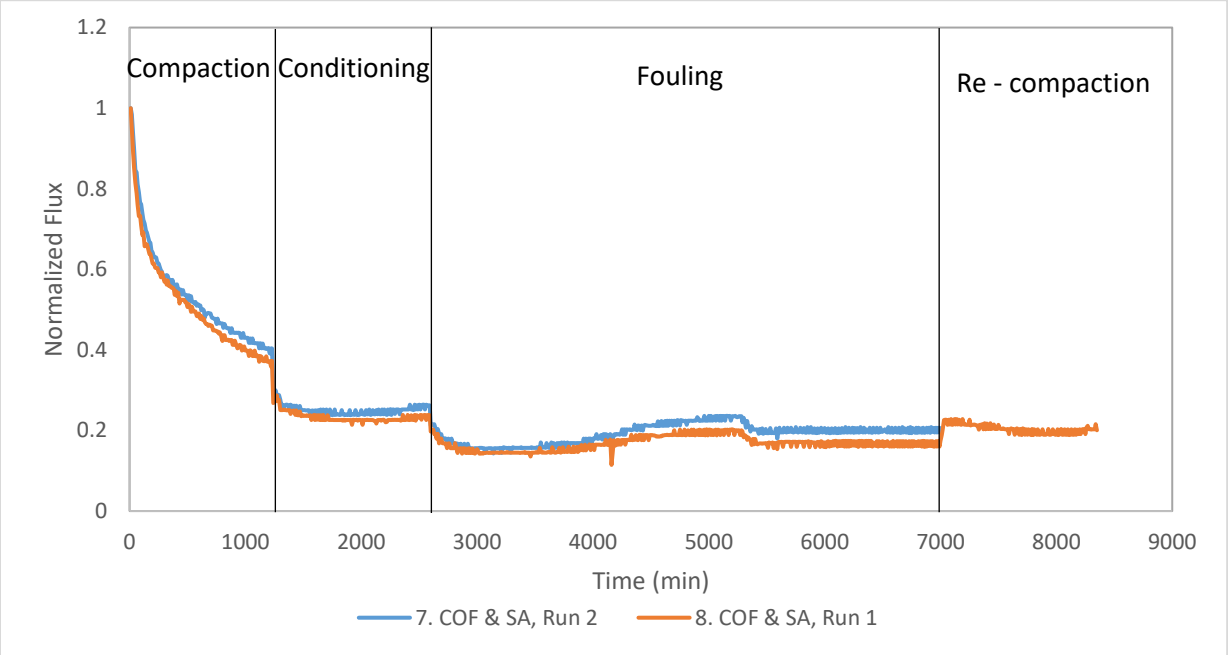

Figure 10. Change in flux over time, normalized by the maximum flux, during organic fouling by 25 mg/L SA in COF membranes. Note these membranes only underwent a 24 hour compaction phase.

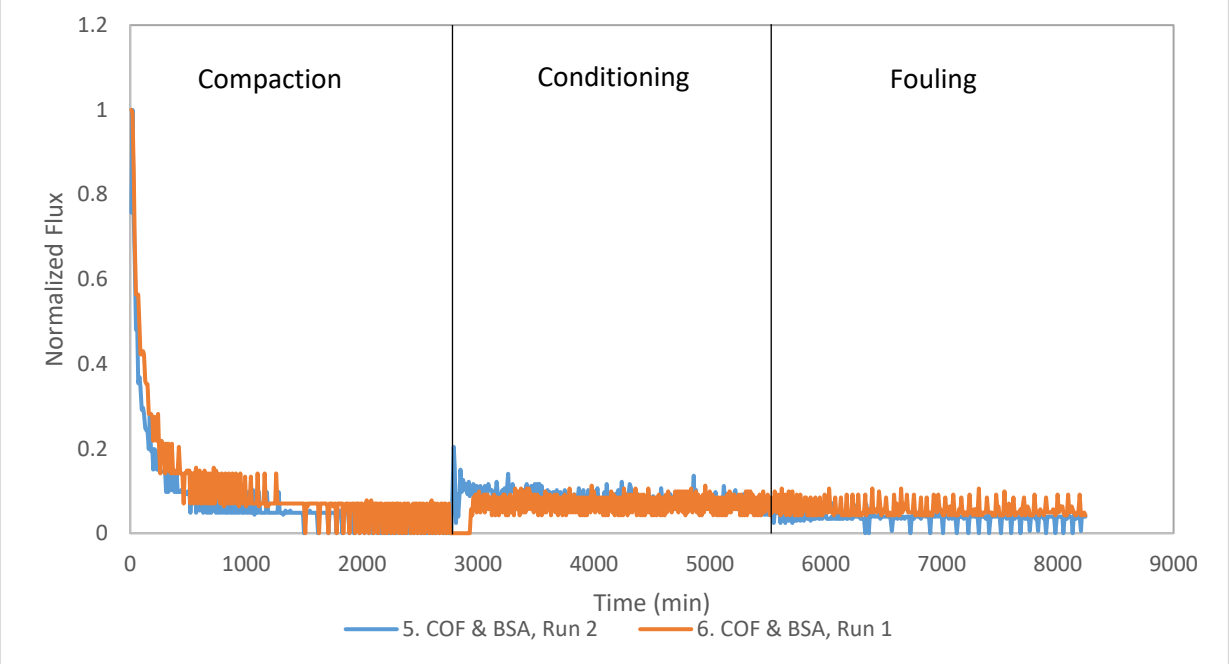

Figure 11. Change in flux over time, normalized by the maximum flux, during organic fouling by 25 mg/L BSA in COF membranes.

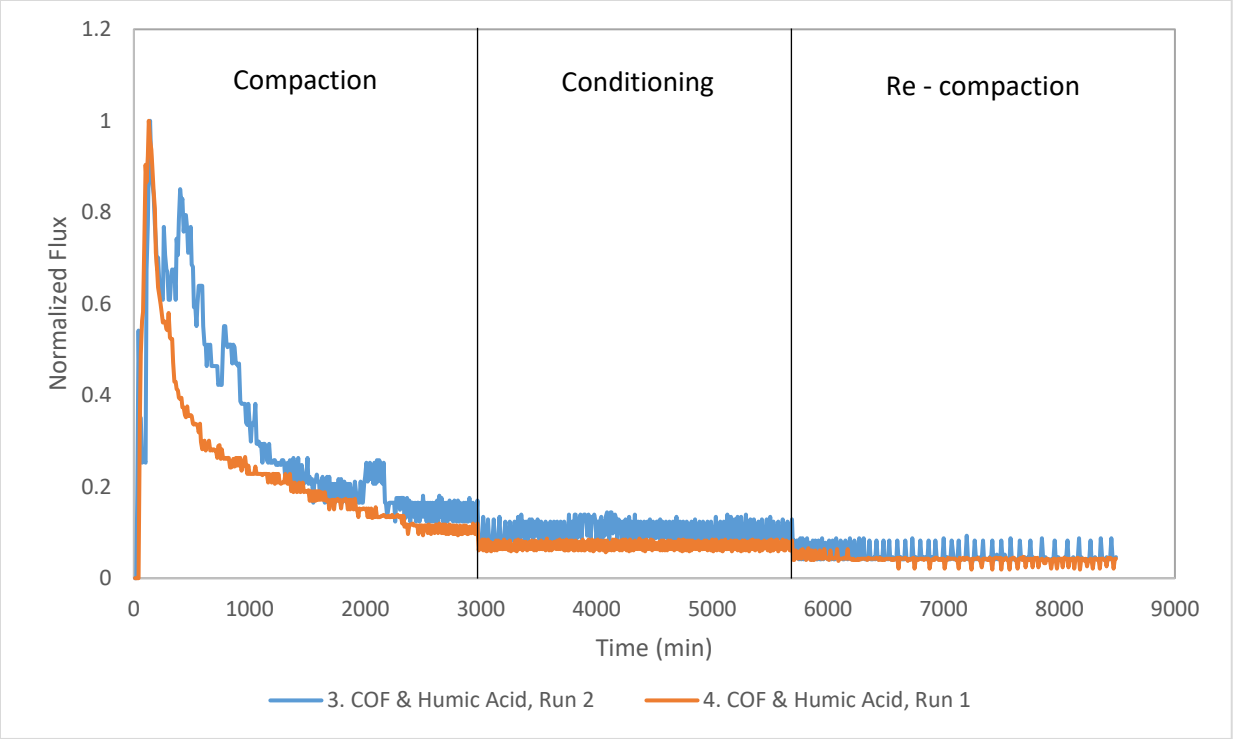

Figure 12. Change in flux over time, normalized by the maximum flux, during organic fouling by 25 mg/L Humic Acid in COF membranes.

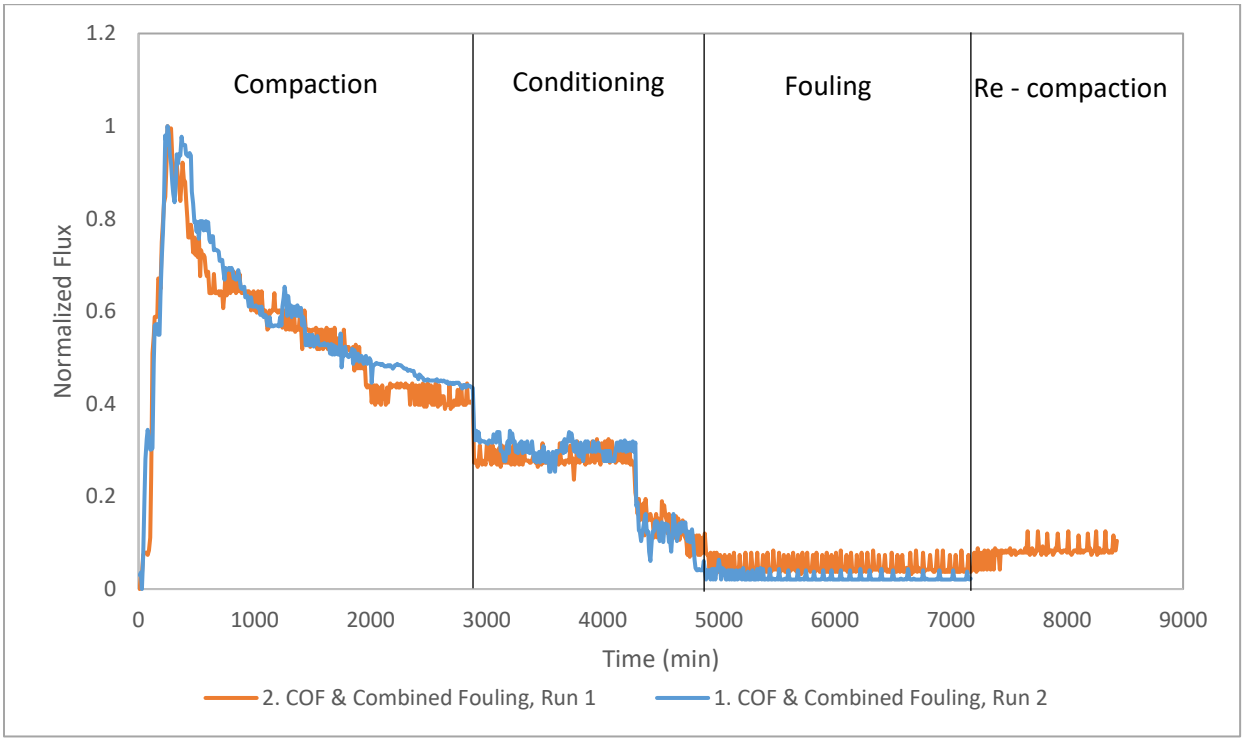

Figure 13. Change in flux over time, normalized by the maximum flux, during organic fouling by 25 mg/L combined fouling solution in COF membranes.

3.4 Fouling Rate

The fouling rate of membranes is the rate at which flux declines over time. This is used to find the average fouling rate over a given period of time. COF membranes fouled with BSA, HA, and the combined fouling solution exhibited rapid fouling in the first 8 hours of the experiment and then fouled at a significantly lower rate throughout the rest remainder of the experiment (Figure 14). Interestingly, the COF membrane fouled with SA exhibited an overall positive fouling rate, and the exact reason was unknown. The first 8 hours had a negative fouling rate greater than the other COF membranes before reaching a steady state (Figure 15). The membranes then experienced roughly 26 hours of fouling that exhibited flux recovery properties before again rapidly fouling and reaching steady state.

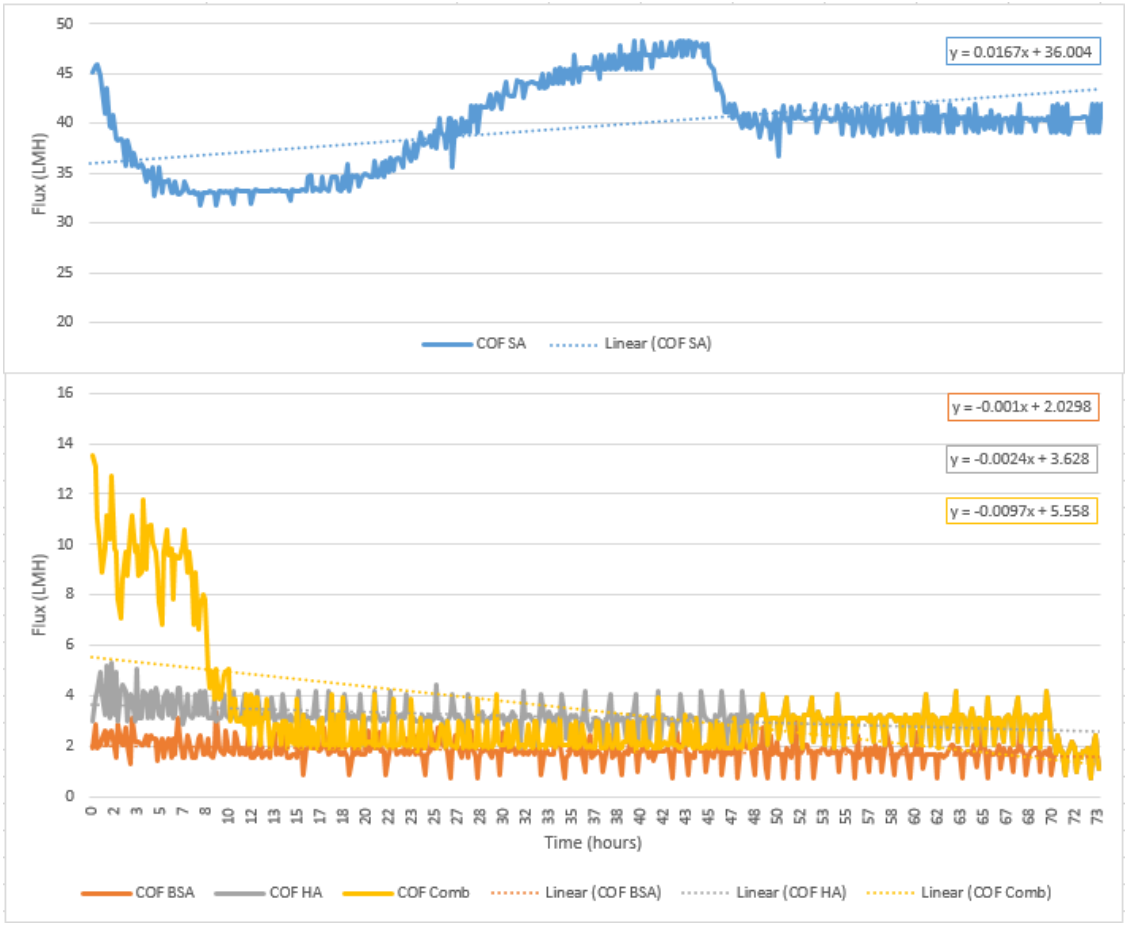

Figure 14. Fouling rate in COF membranes over the full experiment time

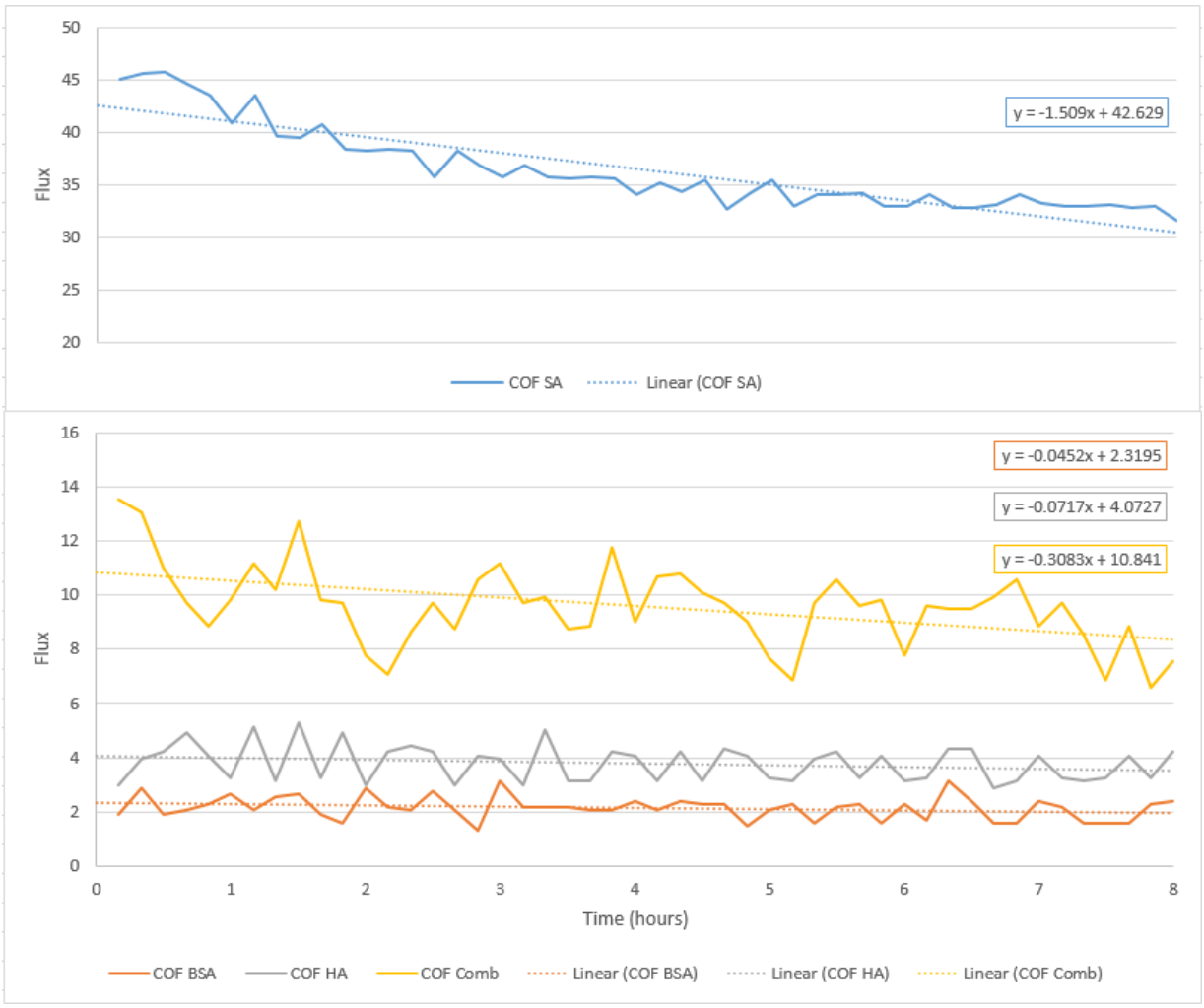

Figure 15. Fouling rate in COF membranes over the first eight hours

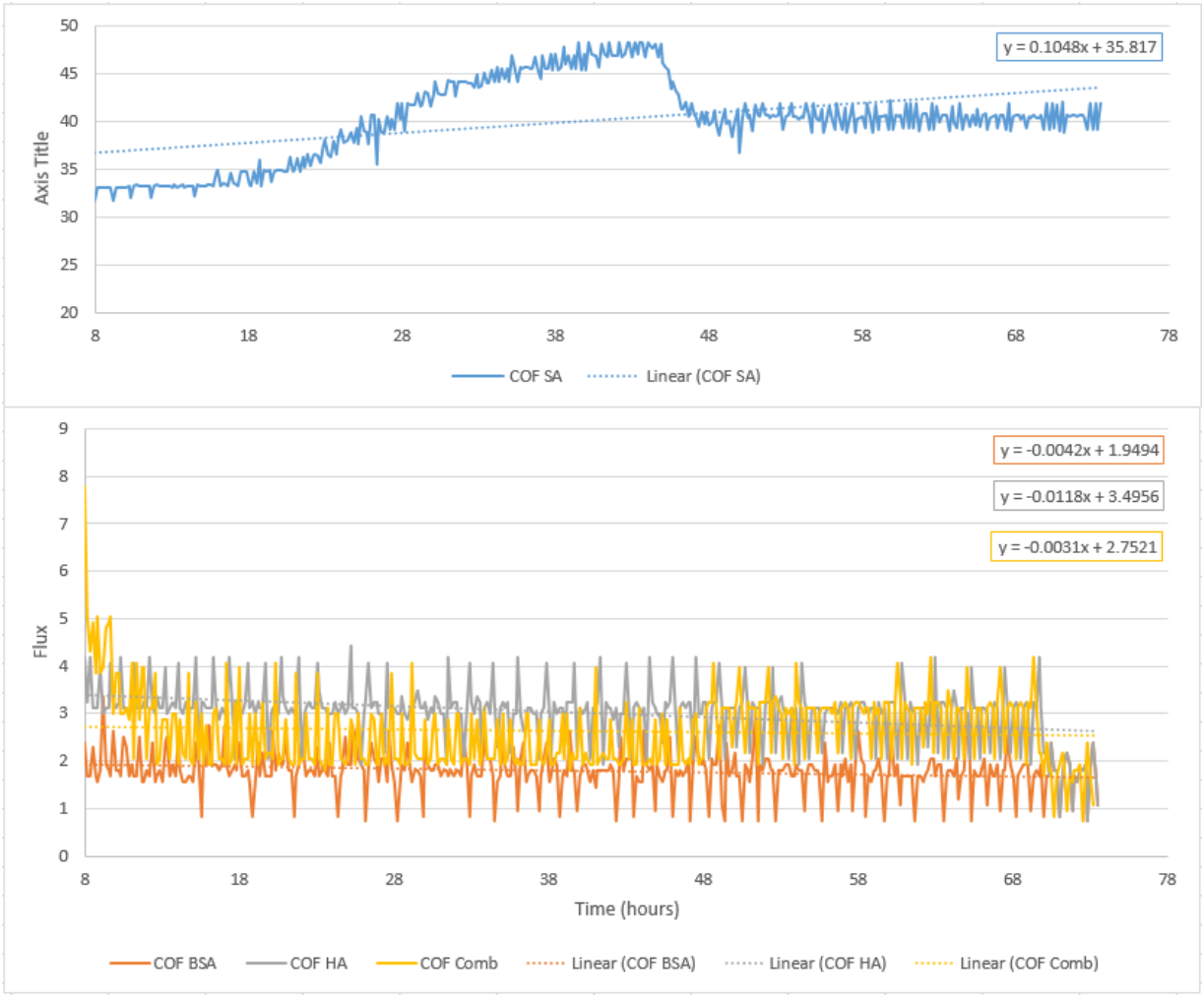

Figure 16. Fouling rate in COF membranes after the first eight hours

In contrast to the COF membranes, NF270 membranes fouled with SA, BSA, HA, and the combined fouling solution exhibited more rapid fouling after the first 8 hours of the experiment compared to the first 8 hours (Figures 17 – 19). Overall, HA exhibited the greatest fouling rate while SA had the slowest fouling rate.

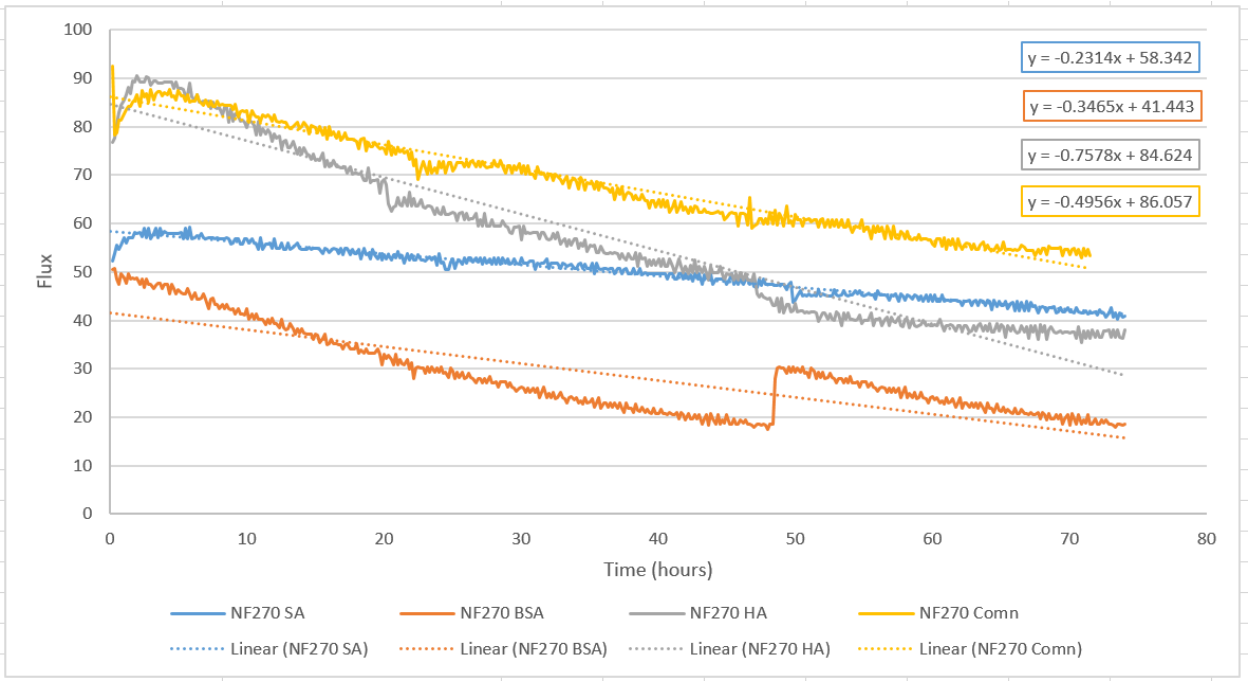

Figure 17. Fouling rate in NF270 membranes over the full experiment time

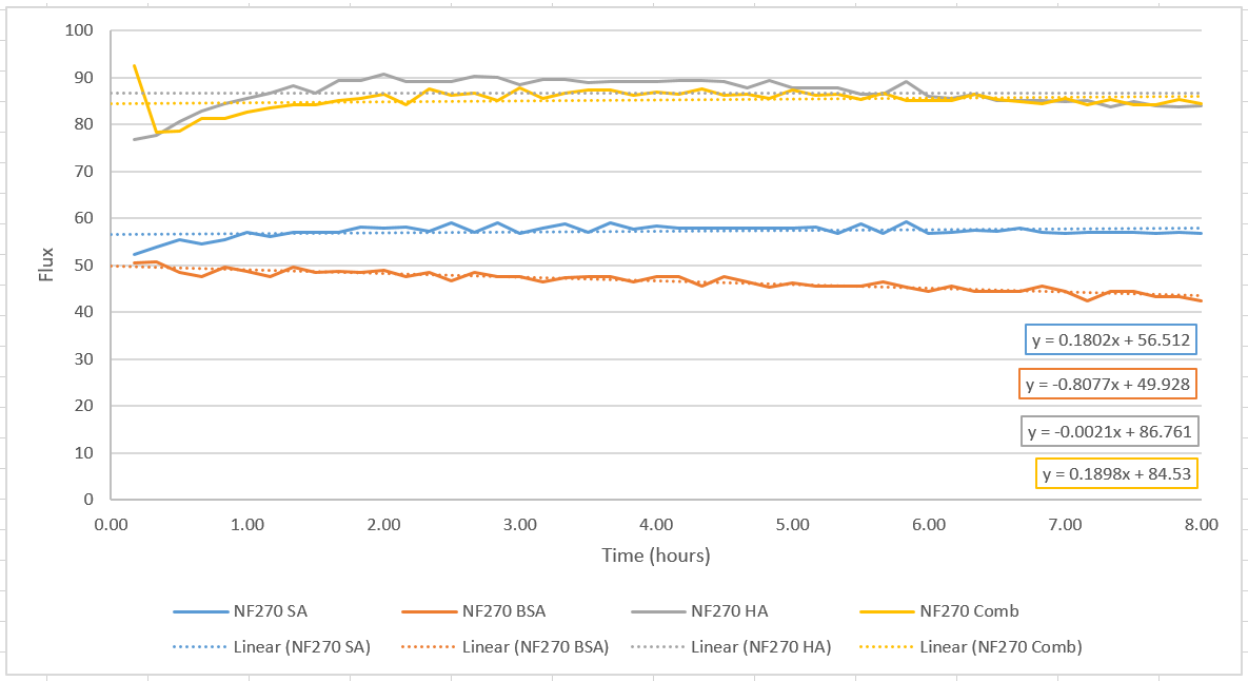

Figure 18. Fouling rate in NF270 membranes over the first eight hours

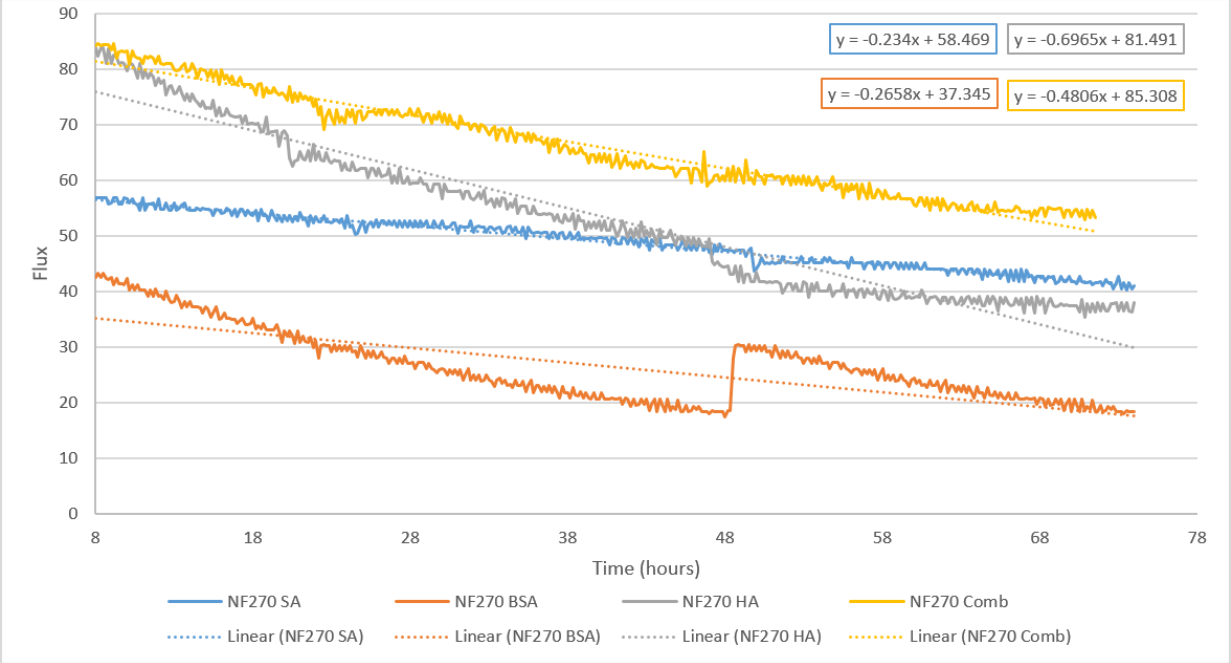

Figure 19. Fouling rate in NF270 membranes after the first eight hours

Overall, the NF270 membranes experienced greater fouling than the COF membranes. For COF membranes, greater fouling was experienced in the first 8 hours while NF270 membranes experienced greater fouling after the first 8 hours.

3.5 Fouling Mechanism Modeling

Fouling mechanism of different foulants can be theoretically modeled. There are single fouling modeling and combined fouling modeling. The single fouling models include standard blocking, complete blocking, intermediate blocking, and cake filtration modeling. Often in natural environments, more than one fouling mechanism is at work. This leads to the development of combined fouling models. The combined fouling models include cake complete, cake intermediate, complete standard, intermediate standard, and cake standard. These theoretical simulations are often applied to better understand which fouling mechanism is most present.

Both single and combined fouling mechanism modeling was performed and compared to the experimental data from the NF270 and COF membranes. The model fit error and model fit variance was calculated and used to evaluate the model that best fit the fouling observed. Based on previous studies, it was hypothesized that the dominant fouling mechanism for SA would be cake filtration due to its gelatinous properties. It was also hypothesized that cake filtration would be the dominant fouling mechanism for BSA, HA, and the combined fouling solution because a foulant layer was observed on the membrane surfaces.

3.5.1 Standard blocking mechanism

The standard blocking mechanism (Equation 3) represents the conditions that allow particles to be deposited on the internal pore wall leading to a decrease in pore volume. The model is generally used to describe the filtration behavior of relatively dilute solutions.

$$V = \left(\frac{1}{J_0 t} + \frac{K_s}{2}\right)^{-1} \quad (3)$$

Where,

J_0 = Initial flux (LMH)

t= Time (hours)

V = volume of permeate (L)

K_s = standard blocking constant (m^{-1})

Table 3. Standard blocking model fit error, model variance, and model fit parameter for all membranes and fouling solutions.

Model	Membrane	Foulant	Model Fit Error, SSR	Model Variance, R2	Fit Parameter Values
Standard Blocking	COF	SA	7.3406	0.4226	3.9237
		BSA	0.0105	0.4783	86.5447
		HA	0.0313	0.4776	49.9810
		Combined	0.0242	0.4817	42.9344
	NF270	SA	8.9118	0.4807	2.9872
		BSA	2.0478	0.5308	5.0699

	HA	17.7411	0.4007	2.2750
	Combined	16.6992	0.3664	2.5714

3.5.2 Complete blocking mechanism

The complete blocking mechanism (Equation 4) represents the conditions in which foulants deposit and accumulate entirely on the membrane surface clogging the membrane pores.

$$V = \frac{J_0}{K_b}(1 - e^{K_b t}) \quad (4)$$

Where,

J_0 = Initial flux (LMH)

t= Time (hours)

V = volume of permeate (L)

K_b = Complete blocking constant ($hour^{-1}$)

Table 4.Complete blocking model fit error, model variance, and model fit parameter for all membranes and fouling solutions.

Model	Membrane	Foulant	Model Fit Error, SSR	Model Variance, R2	Fit Parameter Values
Complete Blocking	COF	SA		Could not fit model	
		BSA		Could not fit model	
		HA		Could not fit model	
		Combined	0.0242	0.481613292	291.1202
	NF270	SA		Could not fit model	
		BSA		Could not fit model	
		HA	17.7537	0.400253613	86.5646
		Combined		Could not fit model	

3.5.3 Intermediate blocking mechanism

The intermediate blocking mechanism (Equation 5) represents the conditions in which foulants deposit within the pores as well as accumulating on the membrane surface causing both pore volume reduction and clogging of the membrane pores.

$$V = \frac{1}{K_i}\ln(1 + K_i J_0 t) \quad (5)$$

Where,

J_0 = Initial flux (LMH)

t= Time (hours)

V = volume of permeate (L)

K_i = Intermediate blocking constant ($hour^{-1}$)

Table 5. Intermediate blocking model fit error, model variance, and model fit parameter for all membranes and fouling solutions.

Model	Membrane	Foulant	Model Fit Error, SSR	Model Variance, R2	Fit Parameter Values
Intermediate Blocking	COF	SA	6.1016	0.5200	20.9054
		BSA	0.0084	0.5836	457.1509
		HA	0.0249	0.5844	261.1889
		Combined	0.0186	0.6022	256.7738
	NF270	SA	7.0884	0.5869	15.6696
		BSA	1.5587	0.6429	28.0585
		HA	13.0568	0.5589	12.2811
		Combined	12.8129	0.5138	14.4749

3.5.4 Cake filtration mechanism

The cake filtration mechanism (Equation 6) represents the conditions in which foulants form a cake layer which increases in size as fouling continues.

$$V = \frac{1}{K_c J_0}(1\sqrt{1 + 2K_c {J_0}^2 t} - 1) \quad (6)$$

Where,

J_0 = Initial flux (LMH)

t= Time (hours)

V = volume of permeate (L)

K_c = Cake filtration constant ($hour/m^2$)

Table 6. Cake filtration model fit error, model variance, and model fit parameter for all membranes and fouling solutions.

Model	Membrane	Foulant	Model Fit Error, SSR	Model Variance, R2	Fit Parameter Values
Cake Filtration	COF	SA	0.2694	0.8365	2748.8522
		BSA	0.0021	0.8980	175807.0530
		HA	0.0008	0.8986	452661.0878
		Combined	0.0019	0.9591	44058.6000
	NF270	SA	Could not fit model		
		BSA	0.0251	0.9557	4776.0039
		HA	1.1489	0.9612	147.8962
		Combined	Could not fit model		

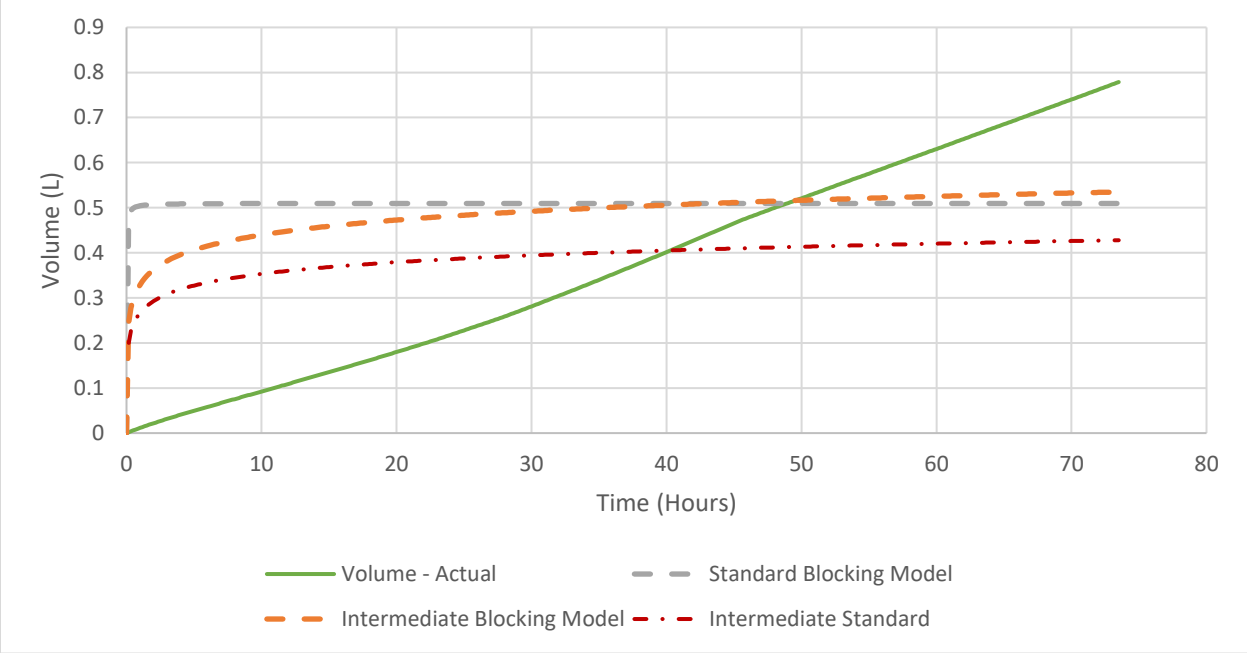

Figure 20. Volume versus time of COF membrane fouled for 24-hours with 25 mg/L of sodium alginate at a constant pressure of 80 psi compared to Standard Blocking, Intermediate Blocking, and Cake Filtration models.

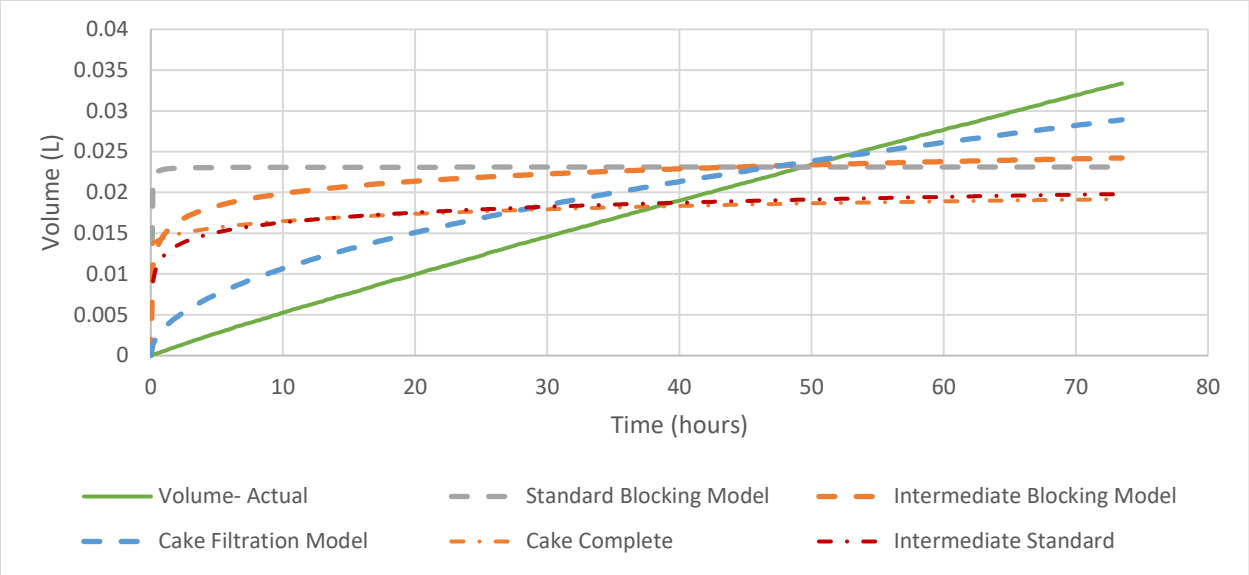

Figure 21. Volume versus time of COF membrane fouled for 24-hours with 25 mg/L of BSA at a constant pressure of 80 psi compared to Standard Blocking, Intermediate Blocking, and Cake Filtration models.

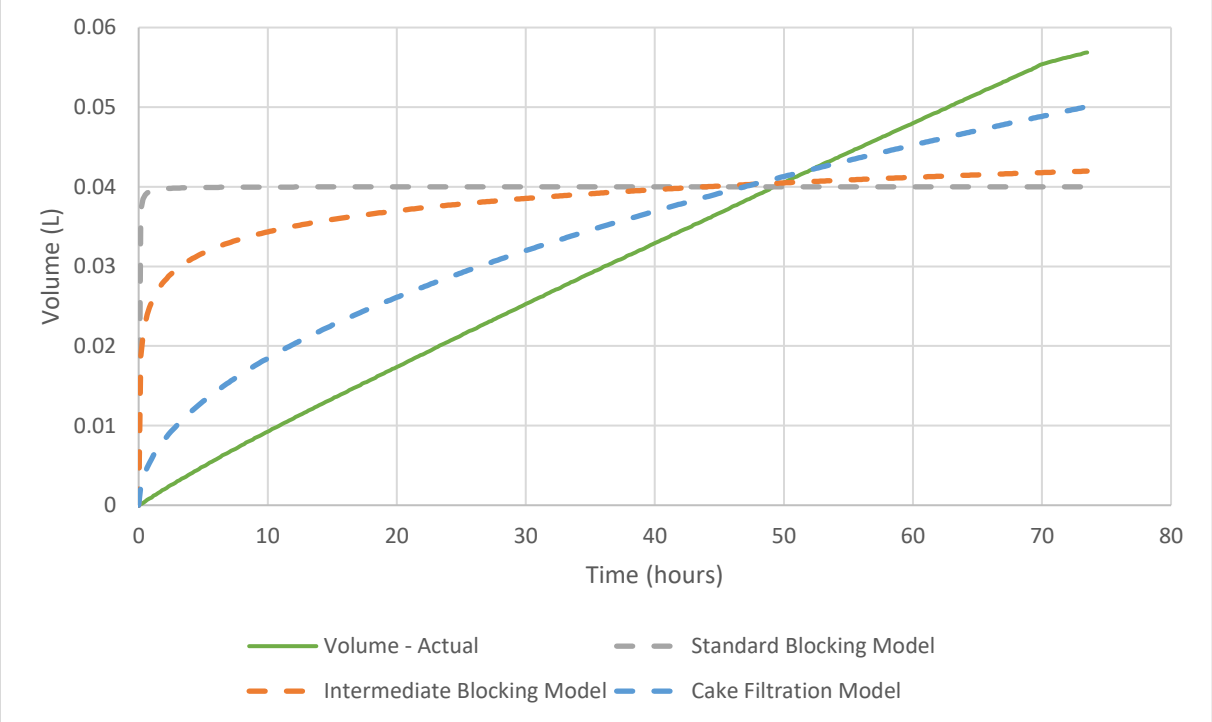

Figure 22. Volume versus time of COF membrane fouled for 24-hours with 25 mg/L of Humic Acid at a constant pressure of 80 psi compared to Standard Blocking, Intermediate Blocking, and Cake Filtration models.

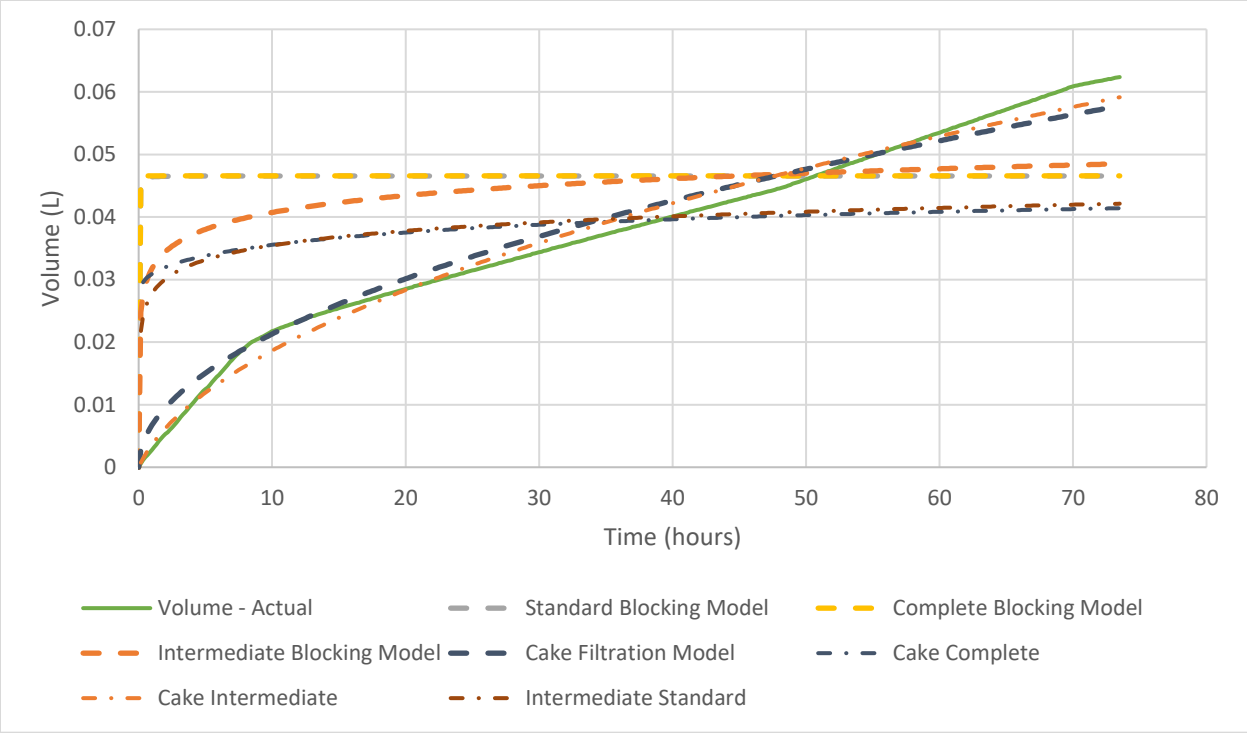

Figure 23. Volume versus time of COF membrane fouled for 24-hours with 25 mg/L of Sodium Alginate, SBA, and Humic Acid at a constant pressure of 80 psi compared to Standard Blocking, Complete Blocking, Intermediate Blocking, and Cake Filtration models.

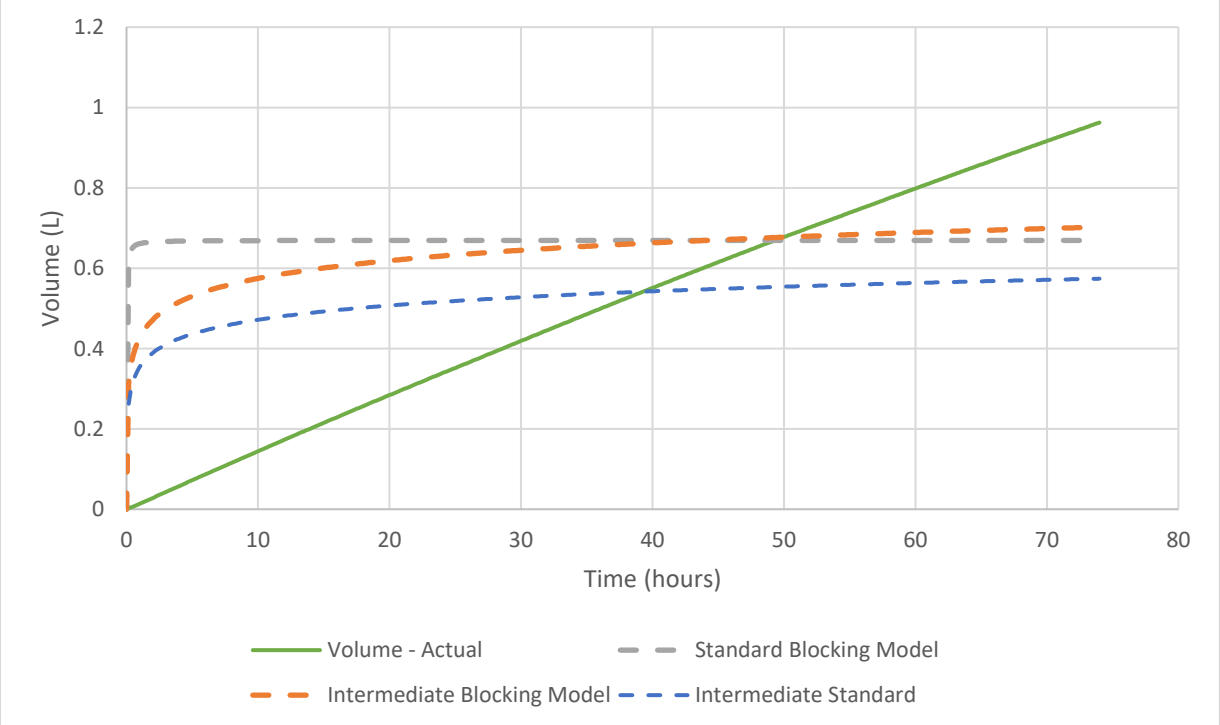

Figure 24. Volume versus time of NF270 membrane fouled for 24-hours with 25 mg/L of sodium alginate at a constant pressure of 80 psi compared to Standard Blocking, Intermediate Blocking, and Cake Filtration models.

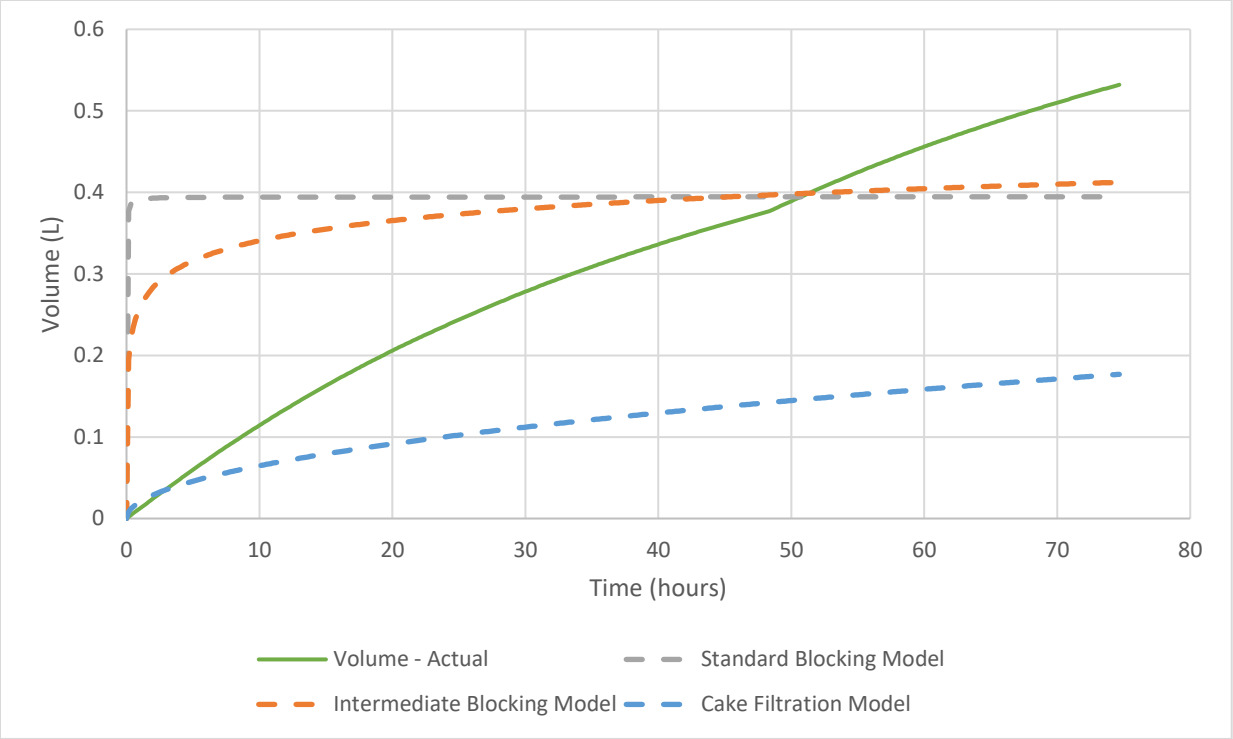

Figure 25. Volume versus time of NF270 membrane fouled for 24-hours with 25 mg/L of BSA at a constant pressure of 80 psi compared to Standard Blocking, Intermediate Blocking, and Cake Filtration models.

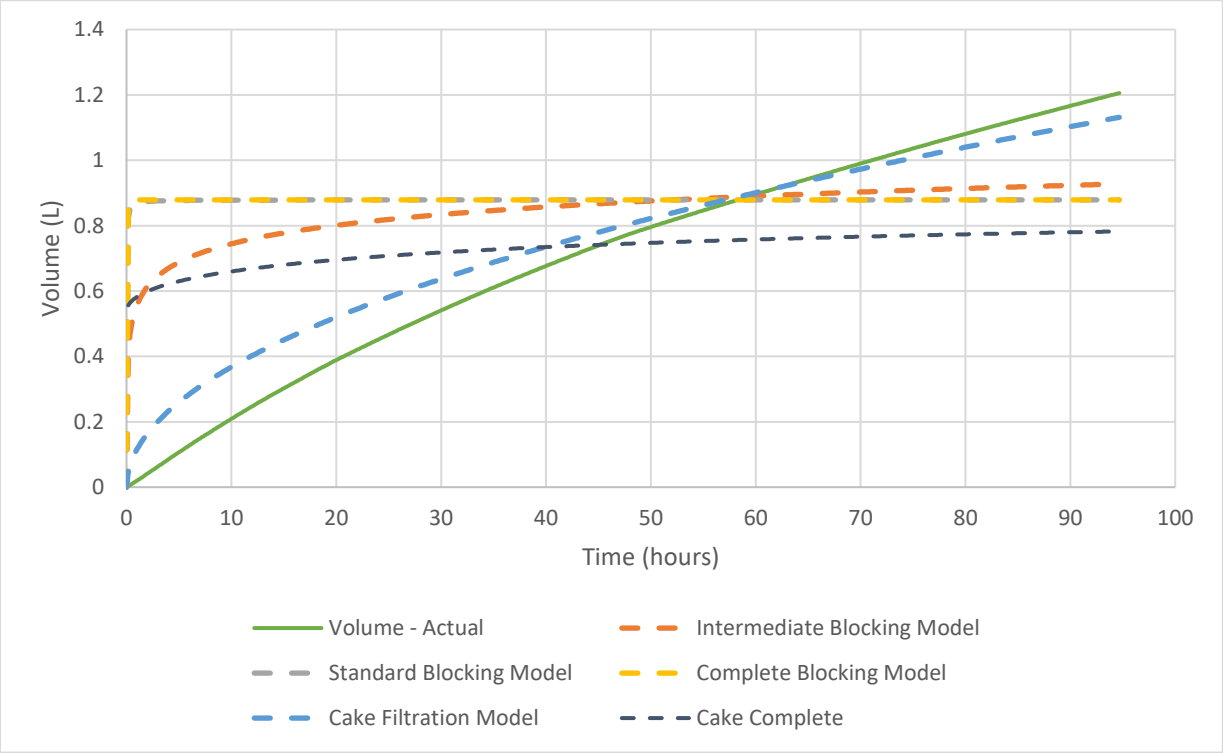

Figure 26. Volume versus time of NF270 membrane fouled for 24-hours with 25 mg/L of Humic Acid at a constant pressure of 80 psi compared to Standard Blocking, Intermediate Blocking, and Cake Filtration models.

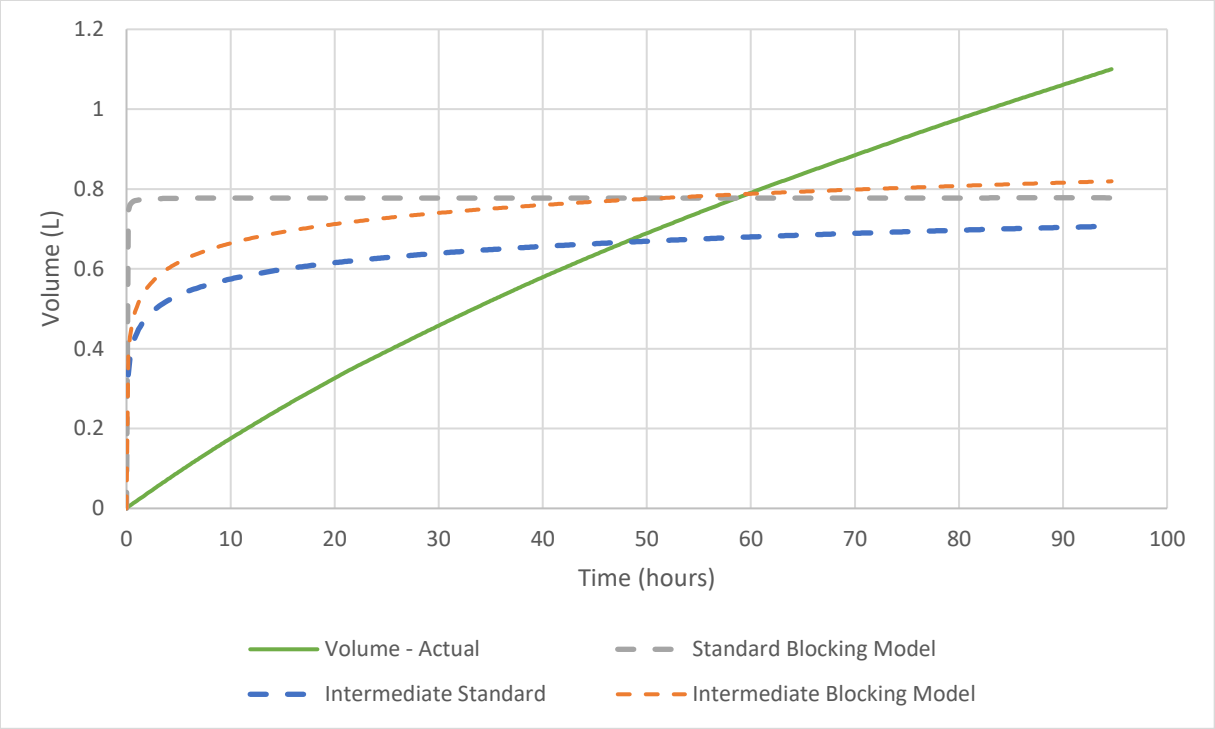

Figure 27. Volume versus time of COF membrane fouled for 24-hours with 25 mg/L of Sodium Alginate, SBA, and Humic Acid at a constant pressure of 80 psi compared to Standard Blocking, Complete Blocking, Intermediate Blocking, and Cake Filtration models.

There were two main dominant fouling models in this study. For all COF membranes, except those fouled with SA, the cake filtration model was the closest to the observed data, yielding R^2 values ranging from 0.989 to 0.987. The intermediate blocking model was the closest to the observed data for COF membranes fouled by SA with an R^2 value of 0.520. For the NF270 membranes, the intermediate blocking model fit the observed data best for membranes fouled with SA, BSA, and the combined foulant fouling solution with R^2 values ranging from 0.514 to 0.643. The cake filtration model was the closest to the observed data for NF270 fouled with humic acid, with an R^2 value of 0.961.

4. Conclusions and Recommendations

4.1 Conclusions

Membrane fouling was observed in all experiments. Two fouling mechanism models were found to be primary fouling mechanisms. Cake filtration was the primary fouling mechanism in the low-permeate COF membranes and the NF270 membrane fouled with HA. For the high-permeate COF membrane and the remaining NF270 membranes, the intermediate blocking model was found to be the primary fouling mechanism. There was limited success in fitting the observed data to the combined fouling mechanism models and in all cases, the single fouling mechanisms were more consistent with the experimental data.

During the COF membrane experiments, a majority of the fouling was observed within the first eight hours of the experiment. During the NF270 membranes, fouling increased after the first eight hours. Overall, due to the difference in membrane permeate flux, it is difficult to draw a fair conclusion as to whether COF or NF270 membranes experienced greater fouling independent of the membranes initial permeate flux. The NF270 membranes were found to have higher initial fluxes than the lab synthesized membranes.

Overall, the lab synthesized COF membranes show a quicker initial fouling than the NF270 membranes, while the NF270 membranes had a greater overall extent of fouling over the experiments. Fouling rates and prominent fouling mechanisms differed between the two sets of membranes. There is limited cross over and similarities between the two groups of membranes tested in the study. Future replicated work is needed to expand and validate the results found in this study.

4.2 Future Work

There are a number of directions in which this research could go to further progress it. Firstly, these experiments can be expanded to include more categories of foulants. It could also be interesting to look at different foulant combinations as well as different concentrations of foulants, and varying pressures. Secondly, the co-existence of cations in the feed solution and at varying concentrations could be explored. The presence of cations like Ca^{2+} and Mg^{2+} has the potential to negate the charge-shielding effect associated with many PFAS molecules. This could cause charge neutralization and increase the affinity for the membrane surface.

It could also be interesting to look at further applications of the single and combined fouling mechanism models, particularly in longer fouling durations and in varying low to high-permeate COF membranes. It would be interesting to see how the dominate fouling mechanism changes as the permeate flux changes in the COF membranes. Additionally, in the event that a combined fouling mechanism model fits the observed data best, it would be interesting to discover when in the fouling process, the combined fouling mechanism become the dominate mechanism over the initial single fouling mechanism.

Once NOM fouling relationships are more thoroughly understood in COF membranes, research could be expanded to explore the impact of NOM on PFAS rejection in COF membranes. Specifically, the research can be expanded to explore the effects of different types and concentrations of NOM, molecular structure, and water chemistry on PFAS removal in COF membranes. Further, research could be replicated and applied to PFAS of varying carbon chain lengths and functional head groups.

References

[1] Sibel Barisci, Rominder Suri; Occurrence and removal of poly/perfluoroalkyl substances (PFAS) in municipal and industrial wastewater treatment plants. *Water Sci Technol* 15 December 2021; 84 (12): 3442–3468. doi: https://doi.org/10.2166/wst.2021.484

[2] Lenka, S. P., Kah, M., & Padhye, L. P. (2021). A review of the occurrence, transformation, and removal of poly- and perfluoroalkyl substances (PFAS) in wastewater treatment plants. *Water Research*, *199*, 117187. https://doi.org/10.1016/j.watres.2021.117187

[3] Yadav, S., Ibrar, I., Al-Juboori, R. A., Singh, L., Ganbat, N., Kazwini, T., Karbassiyazdi, E., Samal, A. K., Subbiah, S., & Altaee, A. (2022). Updated review on Emerging Technologies for pfas contaminated water treatment. *Chemical Engineering Research and Design*, *182*, 667–700. https://doi.org/10.1016/j.cherd.2022.04.009

[4] Rahman, M. F., Peldszus, S., & Anderson, W. B. (2014). Behaviour and fate of perfluoroalkyl and polyfluoroalkyl substances (pfass) in drinking water treatment: A Review. *Water Research*, *50*, 318–340. https://doi.org/10.1016/j.watres.2013.10.045

[5] Domingo, J. L., & Nadal, M. (2019). Human exposure to per- and polyfluoroalkyl substances (PFAS) through drinking water: A review of the recent scientific literature. *Environmental Research*, *177*, 108648. https://doi.org/10.1016/j.envres.2019.108648

[6] Wanninayake, D. M. (2021). Comparison of currently available Pfas Remediation Technologies in water: A Review. *Journal of Environmental Management*, *283*, 111977. https://doi.org/10.1016/j.jenvman.2021.111977

[7] Wang, W., Jia, Y., Zhou, S., & Deng, S. (2023). Removal of typical pfas from water by covalent organic frameworks with different pore sizes. *Journal of Hazardous Materials*, *460*, 132522. https://doi.org/10.1016/j.jhazmat.2023.132522

[8] Li, H., Junker, A. L., Wen, J., Ahrens, L., Sillanpää, M., Tian, J., Cui, F., Vergeynst, L., & Wei, Z. (2023). A recent overview of per- and polyfluoroalkyl substances (PFAS) removal by functional framework materials. *Chemical Engineering Journal*, *452*, 139202. https://doi.org/10.1016/j.cej.2022.139202

[9] Kucharzyk, K. H., Darlington, R., Benotti, M., Deeb, R., & Hawley, E. (2017). Novel treatment technologies for pfas compounds: A critical review. *Journal of Environmental Management*, *204*, 757–764. https://doi.org/10.1016/j.jenvman.2017.08.016

[10] Liu, F., Pignatello, J. J., Sun, R., Guan, X., & Xiao, F. (2024). A comprehensive review of novel adsorbents for per- and polyfluoroalkyl substances in water. *ACS ES&T Water*, *4*(4), 1191–1205. https://doi.org/10.1021/acsestwater.3c00569

[11] Verma, S., Varma, R. S., & Nadagouda, M. N. (2021). Remediation and mineralization processes for per- and polyfluoroalkyl substances (PFAS) in water: A

Review. *Science of The Total Environment*, *794*, 148987. https://doi.org/10.1016/j.scitotenv.2021.148987

[12] Yuan, S., Li, X., Zhu, J., Zhang, G., Van Puyvelde, P., & Van der Bruggen, B. (2019). Covalent organic frameworks for membrane separation. *Chemical Society Reviews*, *48*(10), 2665–2681. https://doi.org/10.1039/c8cs00919h

[13] Xiong, J., Hou, Y., Wang, J., Liu, Z., Qu, Y., Li, Z., & Wang, X. (2021). The rejection of perfluoroalkyl substances by nanofiltration and reverse osmosis: influencing factors and combination processes. *Environmental Science: Water Research & Technology*, *7*(11), 1928-1943.

[14] Lee, T., Speth, T. F., & Nadagouda, M. N. (2022). High-pressure membrane filtration processes for separation of per- and polyfluoroalkyl substances (PFAS). *Chemical Engineering Journal*, *431*, 134023. https://doi.org/10.1016/j.cej.2021.134023

[15] Digambar B. Shinde, Guan Sheng, Xiang Li, Mayur Ostwal, Abdul-Hamid Emwas, Kuo-Wei Huang, and Zhiping Lai Journal of the American Chemical Society 2018 140 (43), 14342-14349 DOI: 10.1021/jacs.8b08788

[16] Lee, T., Speth, T. F., & Nadagouda, M. N. (2022). High-pressure membrane filtration processes for separation of Per- and polyfluoroalkyl substances (PFAS). *Chemical Engineering Journal*, *431*, 134023. https://doi.org/10.1016/j.cej.2021.134023

[17] Liu, C., Zhao, X., Faria, A. F., Deliz Quiñones, K. Y., Zhang, C., He, Q., Ma, J., Shen, Y., & Zhi, Y. (2022). Evaluating the efficiency of nanofiltration and reverse osmosis membrane processes for the removal of per- and polyfluoroalkyl substances from water: A critical review. *Separation and Purification Technology*, *302*, 122161. https://doi.org/10.1016/j.seppur.2022.122161

[18] Liu, C., Shen, Y., Zhao, X., Chen, Z., Gao, R., Zuo, Q., He, Q., Ma, J., & Zhi, Y. (2023). Removal of per- and polyfluoroalkyl substances by nanofiltration: Effect of molecular structure and coexisting natural organic matter. *Journal of Hazardous Materials*, *454*, 131438. https://doi.org/10.1016/j.jhazmat.2023.131438

[19] Mastropietro, T. F., Bruno, R., Pardo, E., & Armentano, D. (2021). Reverse osmosis and nanofiltration membranes for highly efficient PFASs removal: overview, challenges and future perspectives. *Dalton Transactions*, *50*(16), 5398–5410. https://doi.org/10.1039/d1dt00360g

[20] Tow, E. W., Ersan, M. S., Kum, S., Lee, T., Speth, T. F., Owen, C., Bellona, C., Nadagouda, M. N., Mikelonis, A. M., Westerhoff, P., Mysore, C., Frenkel, V. S., deSilva, V., Walker, W. S., Safulko, A. K., & Ladner, D. A. (2021). Managing and treating per- and polyfluoroalkyl substances (PFAS) in membrane concentrates. *AWWA Water Science*, *3*(5). https://doi.org/10.1002/aws2.1233

[21] Boivin, S., & Fujioka, T. (2024). Membrane fouling control and contaminant removal during direct nanofiltration of surface water. *Desalination*, *581*, 117607. https://doi.org/10.1016/j.desal.2024.117607

[22] Ang, W. S., Lee, S., & Elimelech, M. (2006). Chemical and physical aspects of cleaning of organic-fouled reverse osmosis membranes. *Journal of Membrane Science*, *272*(1–2), 198–210. https://doi.org/10.1016/j.memsci.2005.07.035

[23] Li, Z., Zheng, Y., Gu, T., Meng, X., Wang, H., Xu, K., Cheng, L., Kasher, R., Zhang, R., & Jiang, Z. (2023). Covalent organic framework membrane with sub-nano pores for efficient desalination. *Journal of Membrane Science*, *675*, 121551. https://doi.org/10.1016/j.memsci.2023.121551

[24] Son, H., Kim, T., Yoom, H. S., Zhao, D., & An, B. (2020). The Adsorption Selectivity of Short and Long Per- and Polyfluoroalkyl Substances (PFASs) from Surface Water Using Powder-Activated Carbon. *Water*, *12*(11), 3287. https://doi.org/10.3390/w12113287

[25] BOLTON, G., LACASSE, D., & KURIYEL, R. (2006). Combined models of membrane fouling: Development and application to microfiltration and ultrafiltration of biological fluids. *Journal of Membrane Science*, *277*(1–2), 75–84. https://doi.org/10.1016/j.memsci.2004.12.053

[26] J. Hermia, "Constant pressure blocking filtration laws – application to power-law non-newtonian fluids," *Institution of Chemical Engineers*, vol. 60, pp. 183-187, 1982.

[27] Olimattel, K., Zhai, L., & Sadmani, A. A. (2021). Enhanced removal of perfluorooctane sulfonic acid and perfluorooctanoic acid via polyelectrolyte functionalized ultrafiltration membrane: Effects of membrane modification and water matrix. *Journal of Hazardous Materials Letters*, *2*, 100043. https://doi.org/10.1016/j.hazl.2021.100043

[28] Das, S., & Ronen, A. (2022). A Review on Removal and Destruction of Per- and Polyfluoroalkyl Substances (PFAS) by Novel Membranes. *Membranes*, *12*(7), 662. https://doi.org/10.3390/membranes12070662

[29] Liu, Q., Xu, G.-R., & Das, R. (2019). Inorganic scaling in reverse osmosis (RO) desalination: Mechanisms, monitoring, and inhibition strategies. *Desalination*, *468*, 114065. https://doi.org/10.1016/j.desal.2019.07.005

[30] Jiang, S., Li, Y., & Ladewig, B. P. (2017). A review of reverse osmosis membrane fouling and control strategies. *The Science of the Total Environment*, *595*, 567–583. https://doi.org/10.1016/j.scitotenv.2017.03.235

[31] Zhi, Y., Zhao, X., Qian, S., Faria, A. F., Lu, X., Wang, X., Li, W., Han, L., Tao, Z., He, Q., Ma, J., & Liu, C. (2022). Removing emerging perfluoroalkyl ether acids and fluorotelomer sulfonates from water by nanofiltration membranes: Insights into

performance and underlying mechanisms. *Separation and Purification Technology*, *298*, 121648-.

[32] Pang, H., Allinson, M., Northcott, K., Schultz, A., & Scales, P. J. (2023). Demonstrating removal credits for contaminants of emerging concern in recycled water through a reverse osmosis barrier–A predictive framework. *Water Research*, *244*, 120427–120427. https://doi.org/10.1016/j.watres.2023.120427

[33] Boo, C., Wang, Y., Zucker, I., Choo, Y., Osuji, C. O., & Elimelech, M. (2018). High Performance Nanofiltration Membrane for Effective Removal of Perfluoroalkyl Substances at High Water Recovery. *Environmental Science & Technology*, *52*(13), 7279–7288.

[34] Gagliano, E., Sgroi, M., Falciglia, P. P., Vagliasindi, F. G. A., & Roccaro, P. (2020). Removal of poly- and perfluoroalkyl substances (PFAS) from water by adsorption: Role of PFAS chain length, effect of organic matter and challenges in adsorbent regeneration. *Water Research*, *171*, 115381. https://doi.org/10.1016/j.watres.2019.115381

[35] Léniz-Pizarro, F., Vogler, R. J., Sandman, P., Harris, N., Ormsbee, L., Liu, C., & Bhattacharyya, D. (2022). Dual-Functional Nanofiltration and Adsorptive Membranes for PFAS and Organics Separation from Water. *ACS ES&T Water*, *2*(5), 863–872. https://doi.org/10.1021/acsestwater.2c00043

[36] Malaeb, L., & Ayoub, G. M. (2011). Reverse osmosis technology for water treatment: State of the art review. *Desalination*, *267*(1), 1–8. https://doi.org/10.1016/j.desal.2010.09.001

[37] Al-Amoudi, A., & Lovitt, R. W. (2007). Fouling strategies and the cleaning system of NF membranes and factors affecting cleaning efficiency. *Journal of Membrane Science*, *303*(1-2), 4–28. https://doi.org/10.1016/j.memsci.2007.06.002

[38] Buck, R.C., Franklin, J., Berger, U., Conder, J.M., Cousins, I.T., de Voogt, P., Jensen, A.A., Kannan, K., Mabury, S.A. and van Leeuwen, S.P. (2011), Perfluoroalkyl and polyfluoroalkyl substances in the environment: Terminology, classification, and origins. Integr Environ Assess Manag, 7: 513-541. https://doi.org/10.1002/ieam.258

[39] Shivakoti, B. R., Tanaka, S., Fujii, S., Kunacheva, C., Boontanon, S. K., Musirat, C., Seneviratne, S. T. M. L. D., & Tanaka, H. (2010). Occurrences and behavior of perfluorinated compounds (PFCs) in several wastewater treatment plants (WWTPs) in Japan and Thailand. *Journal of Environmental Monitoring*, *12*(6), 1255. https://doi.org/10.1039/b927287a

[40] Zhang, Y., Thomas, A., Onur Apul, & Venkatesan, A. K. (2023). Coexisting ions and long-chain per- and polyfluoroalkyl substances (PFAS) inhibit the adsorption of short-chain PFAS by granular activated carbon. *Journal of Hazardous Materials*, *460*, 132378–132378. https://doi.org/10.1016/j.jhazmat.2023.132378